The role of Task3 potassium channels in the regulation of aldosterone secretion in the adrenal gland

DISSERTATION

ZUR ERLANGUNG DES DOKTORGRADES DER NATURWISSENSCHAFTEN (DR. RER. NAT.) DER FAKULTÄT FÜR BIOLOGIE UND VORKLINISCHE MEDIZIN DER UNIVERSITÄT REGENSBURG

vorgelegt von
David Pentón Ribas
aus La Habana, Cuba

im Jahr 2011

Das Promotionsgesuch wurde eingereicht am: 30.05.2011

Die Arbeit wurde angeleitet von: Prof. Dr. Richard Warth

Prüfungsausschuss:

Vorsitzender:	Prof. Dr. Reinhard Wirth
1. Gutachter:	Prof. Dr. Richard Warth
2. Gutachter:	Prof. Dr. Karl Kunzelmann
3. Gutachter:	Prof. Dr. Stephan Schneuwly
Ersatzperson:	Prof. Dr. Hayo Castrop

Summary

About 10% of the patients suffering from arterial hypertension present abnormal production of aldosterone by the adrenal gland. Cell depolarization is a pivotal event in triggering aldosterone secretion in adrenal *zona glomerulosa* cells when stimulated by angiotensin II and hyperkalemia. These cells, which are strongly hyperpolarized under physiological conditions, have a unique potassium sensitivity conferred by the 2-pore domain potassium channels Task3, Task1 and Trek1. In mice, the deletion of either Task1 or both Task1 and Task3 genes lead to a phenotype which resembles human primary hyperaldosteronism. This study was aimed at investigating the particular contribution of Task3 potassium channels to the regulation of aldosterone production. The adrenal gland was identified as a primary organ of Task3 expression, where Task3-specific immunofluorescence was detected in *zona glomerulosa* cells. In male mice, the sex hormone testosterone promotes the expression of Task3 also in corticosterone-producing cells from *zona fasciculata*. The deletion of Task3 gene caused an impairment of the regulation of aldosterone secretion *in vivo* under high potassium diet. In *ex vivo* experiments using perifused adrenal gland tissue, small changes in the K^+ dependence of aldosterone secretion were observed. Patch clamp analysis on adrenocortical primary cells of Task3 knockout ($Task3^{-/-}$) animals showed a more depolarized membrane voltage, under resting conditions, when compared to wild type ($Task3^{+/+}$) cells. The electrical properties and cytoplasmic Ca^{2+} responses to increasing extracellular K^+ concentration were drastically changed in primary cultures from $Task3^{-/-}$ adrenocortical cells. The stimulation of $Task3^{-/-}$ adrenal primary cells with angiotensin II triggered a paradoxical hyperpolarization instead of the classical depolarization found in $Task3^{+/+}$ cells. In adrenal gland slices from $Task3^{-/-}$ animals the physiological regulation of cytosolic Ca^{2+} signaling appeared to be disturbed. The aldosterone/renin ratio was significantly higher in $Task3^{-/-}$ animals when compared to $Task3^{+/+}$ animals. This finding suggests that the disruption of Task3 leads to partial autonomy in the secretion of aldosterone by the adrenal gland. Altogether these data demonstrate that Task3 potassium channels are important for the normal regulation of aldosterone secretion in the adrenal glands. A defect in the function of these channels could have implications for human disorders linked to pathological production of aldosterone.

Zusammenfassung

Etwa 10% der Patienten mit Bluthochdruck zeigen krankhafte Veränderungen der Aldosteronproduktion in der Nebenniere. Die Depolarisation ist ein entscheidender Schritt für die Induzierung der Aldosteronausschüttung in adrenalen Zellen der *Zona Glomerulosa* nach Stimulation mit Angiotensin II oder durch Hyperkaliämie. Diese Zellen sind unter physiologischen Bedingungen stark hyperpolarisiert und weisen eine einzigartige Kaliumempfindlichkeit auf, welche durch die 2-Poren-domänen Kaliumkanäle Task3, Task1 und Trek1 vermittelt wird. In Mäusen ruft sowohl die Gendeletion von Task1, als auch von Task1 und Task3 gemeinsam, einen Phänotyp ähnlich dem humanen primären Hyperaldosteronismus hervor. In dieser Studie wurde der spezifische Anteil von Task3 Kaliumkanälen an der Regulation der Aldosteronproduktion untersucht. Die Nebenniere wurde als das Organ mit der höchsten Expression von Task3 identifiziert. Immunfluoreszenzfärbungen detektierten Task3 spezifisch in Zellen der *Zona Glomerulosa*. In männlichen Mäusen fördert das Geschlechtshormon Testosteron zusätzlich die Expression von Task3 in Corticosteron produzierenden Zellen der *Zona Fasciculata*. Die Gendeletion von Task3 verursachte eine Störung der *in vivo* Regulation der Aldosteronsekretion durch eine Hochkaliumdiät. In *ex vivo* Experimenten an perifundiertem Nebennierengewebe wurden geringe Änderungen der Kaliumabhängigkeit der Aldosteronsekretion beobachtet. Patch-clamp Experimente zeigen unter Kontrollbedingungen bei primären adrenokortikalen Zellen aus Task3-knockout ($Task3^{-/-}$) Tieren verglichen mit solchen aus Wildtyptieren ($Task3^{+/+}$) ein depolarisiertes Membranpotential. Die elektrophysiologischen Eigenschaften und die zytoplasmatische Ca^{2+} Antwort primär kultivierter $Task3^{-/-}$ adrenokortikaler Zellen in Abhängigkeit ansteigender extrazellulärer Kaliumkonzentration wurden drastisch verändert. Die Stimulation primärer adrenaler $Task3^{-/-}$ Zellen mit Angiotensin II löste, anstatt der klassischen Depolarisation wie man sie in $Task3^{+/+}$ Zellen findet, eine paradoxe Hyperpolarisation aus. In frischen Nebennierenschnitten von $Task3^{-/-}$ Tieren schien die physiologische Regulation des zytosolischen Ca^{2+} Signals gestört zu sein. Der Aldosteron/Renin-Quotient war in $Task3^{-/-}$ Tieren signifikant höher als in $Task3^{+/+}$ Tieren. Dieser Umstand lässt auf eine teilweise Autonomie der Aldosteronsekretion durch die Nebenniere aufgrund der Task3-Deletion schließen. Insgesamt unterstreichen diese Daten, wie wichtig Task3 Kaliumkanäle für die normale Regulation der Aldosteronsekretion sind. Eine

Fehlfunktion dieser Kanäle könnte entscheidend für Erkrankungen des Menschen sein, welche mit einer pathologischen Aldosteronproduktion einhergehen.

Table of contents

Abbreviations

aa	amino acid
ACE	Angiotensin converting enzyme
ACTH	Adrenocorticotropic hormone
AM	Acetoxymethyl ester
AngII	Angiotensin II
ANP	Atrial natriuretic peptide
AT1	Angiotensin II receptor type 1
au	arbitrary units
ATP	Adenosine triphosphate
BSA	Bovine serum albumin
$[Ca^{2+}]_i$	Intracellular Ca^{2+} concentration
CaM	Calmodulin
CaMKs	Calmodulin-dependent kinases
CC0	Current clamp 0
cDNA	complementary deoxyribonucleic acid
CMV	Cytomegalovirus promoter
C-term	Carboxy terminus
Dab2	Disabled-2
DAG	Diacylglycerol
DMEM	Dulbecco's modified Eagle's medium
DNA	Deoxyribonucleic acid
DT	Diphtheria toxin
EGTA	Ethylene glycol tetra acetic acid
ELISA	Enzyme-linked immunosorbent assay
ENaC	Epithelial Na^+ channel
ER	Endoplasmic reticulum
ES	Embryonic stem
EST	Expressed sequence tags
Ex	Exon
GmbH	(in German) Gesellschaft mit beschränkter Haftung
GTP	Guanosine-5'-triphosphate
HEPES	4-(2-Hydroxyethyl)piperazine-1-ethanesulfonic acid
HUGO	Human Genome Organization

IP_3	Inositol 1,4,5-trisphosphate
IU	International units
IUP	International Union of Pharmacology
$[K^+]_o$	Extracellular concentration of K^+
kDa	Kilo Dalton
K_2P	Two pore domains potassium channels
M	Mega or mol/l
m	Milli or metre or murine
MAPKs	Mitogen-activated protein kinases
MaxiK	Large conductance Ca^{2+} activated K^+ channel
min	minute(s)
MR	Mineralocorticoid receptor
mRNA	messenger ribonucleic acid
n	nano, number
NCC	Na^+/Cl^- co-transporter
NHE	Na^+/H^+ exchanger
NKCC2	$Na^+/K^+/2Cl^-$ co-transporter isoform 2
OCT	Optimal cutting temperature
p	Pico
PA	Primary hyperaldosteronism
PBS	Phosphate buffered saline
PCR	Polymerase chain reaction
PFA	Paraformaldehyde
PKA	cAMP-dependent protein kinase A
PKC	Protein kinase C
PLC	Phospholipase C
PMCA	Plasma membrane Ca^{2+} ATPase
PRA	Plasma renin activity
RAS	Renin-Angiotensin System
RIA	Radioimmunoassay
ROMK	Renal outer medullary K^+ channel (KCNJ1)
RT	Reverse transcriptase or room temperature or real-time
SCP2	Sterol carrier protein-2
SEM	Standard error of the mean

SERCA	Sarco/endoplasmic Ca^{2+} ATPase
SGK1	Serum and Glucocorticoid inducible Kinase isoform 1
StAR	Steroidogenic acute regulatory protein
STIM	Stromal interaction molecules
TALK	TWIK-related alkaline pH activated K^+ channel
Task	TWIK-related acid-sensitive K^+ channel
$Task1^{-/-}$	Task1 knockout mouse
$Task1^{-/-}/Task3^{-/-}$	Task1 and Task3 double knockout mouse
$Task3^{-/-}$	Task3 knockout mouse
$Task3^{+/+}$	Wild type mouse (genetic background of $Task3^{-/-}$)
THIK	Tandem pore domains halothane-inhibited K^+ channel
TK	Thymidine kinase
TMS	Transmembrane segment
TRAAK	TWIK-related arachidonic acid-stimulated K^+ channel
TREK	TWIK related K^+ channel
TRESK	Twik-related spinal cord K^+ channel
TRP 4	Transient receptor potential protein 4
TWIK	Tandem of P domains in a weak inwardly rectifying K^+ channel
V	Volt, voltage,
V_c	Voltage clamp
V_m	membrane voltage
WNK	With no lysine (K) kinase
ZF	*Zona fasciculata*
ZG	*Zona glomerulosa*
ZR	*Zona reticularis*
ZX	Zona X

1. Introduction

1 Introduction

Hypertension is a major risk factor in the development of cardiovascular diseases. Approximately 26% of the adult population worldwide had hypertension in 2000 and by 2025 it is predicted that 29% will be affected (1). Although idiopathic hypertension, the term used for unknown causes of this condition, accounts for the majority of the cases, about 1 in 10 hypertensive patients present adrenal primary hyperaldosteronism (PA) (2-4). PA was first described by J Conn in 1955 and has been recently redefined as “a group of disorders in which aldosterone production is inappropriately high, relatively autonomous from the renin-angiotensin system (RAS), and nonsuppressible by sodium loading” (5). The inappropriate production of aldosterone can cause sodium retention, suppression of plasma renin and increased potassium excretion, which when prolonged can lead to hypokalemia. Aldosterone is produced in the adrenal glands and its secretion is stimulated by high plasma potassium concentrations (hyperkalemia) and angiotensin II (AngII) under normal conditions.

1.1 Adrenal glands

The circulating mineralocorticoid aldosterone is primarily produced in the adrenal glands, although the brain (6) and the heart (7) have also been reported to produce it to some extent. In humans, the adrenal glands are situated on top of each kidney, encapsulated and surrounded by adipose tissue. They are comprised of two morphological well differentiated regions that are at the same time two functionally distinct organs: the adrenal medulla and the adrenal cortex. The medulla, derived from neural crest cells, is mainly formed by chromaffin cells and is responsible for the synthesis of the catecholamines adrenalin and noradrenalin. On the other hand, the cortex -which derives from the cells of the intermediate mesoderm- comprises three concentrically distributed zones secreting different steroid hormones: androgens are secreted in the *zona reticularis*; glucocorticoids (mainly cortisol in humans and corticosterone in mice) in the *zona fasciculata* and the mineralocorticoid aldosterone in the *zona glomerulosa* (Figure 1.1). Due to the lack of expression of 17α-hydroxylase, mice and rats do not have the *zona reticularis* found in humans and other mammals; thus they do not secrete adrenal androgens (8). The innermost layer of the adult mice adrenal cortex is called *zona X* and its function is not fully clear (9).

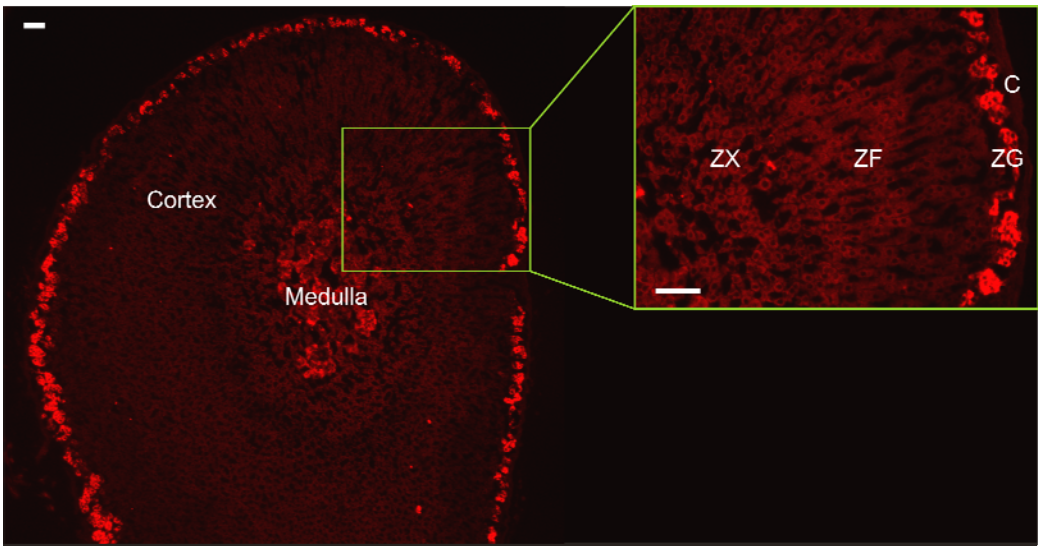

Figure 1.1. Section of the mouse adrenal gland where cortex and medulla are distinguishable (left panel). At a higher magnification (right panel) the red staining corresponds to the specific marker of *zona glomerulosa* (**ZG**) aldosterone synthase **ZF**, **ZX** and **C** are *zona fasciculata*, *zona X* and capsule respectively. Scale bars correspond to 50 µm.

In humans and rodents, functional zonation relies in part on the specific expression of two cytochrome P450 isozymes termed 11β-hydroxylase (the product of the gene CYP11B1) and aldosterone synthase (the product of the gene CYP11B2). These enzymes catalyze the final steps in the biosynthesis of cortisol in humans (or corticosterone in mice) and aldosterone, respectively. Thus, *zona glomerulosa* cells specifically express aldosterone synthase, whereas in *zona fasciculata* cells 11β-hydroxylase is present.

1.1.1 Biosynthesis of aldosterone

As steroid producing cells do not store hormones, the rate of hormone secretion depends fundamentally on their *de novo* synthesis. Cholesterol, the precursor of steroids hormones, may be either synthesized intracellularly from acetyl-coenzyme A or taken up from plasma lipoproteins through receptor mediated endocytosis. In steroid producing cells it can then be stored directly into cytoplasmic lipid droplets or converted to free cholesterol and used for hormone synthesis. A schematic overview of the aldosterone biosynthetic pathway is shown in Figure 1.2.

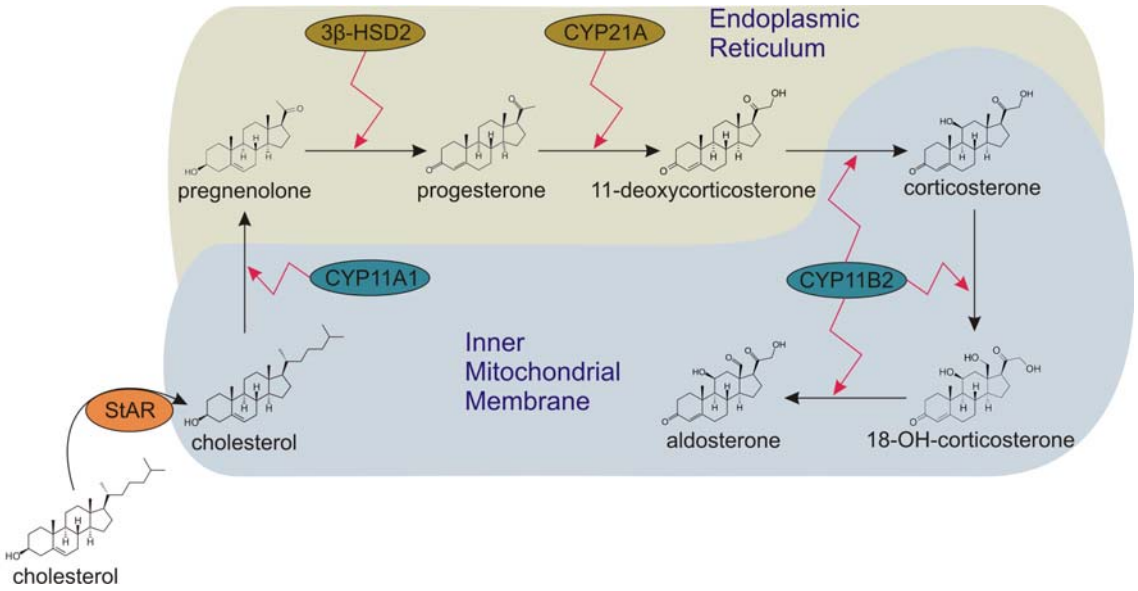

Figure 1.2. Schematic overview of the aldosterone biosynthetic pathway. Red arrows indicate enzymatic activities. The transport of free cholesterol from cytoplasmic lipid droplets to the outer mitochondrial membrane is accomplished by the sterol carrier protein-2 (SCP2) (10). After the translocation of cholesterol from the outer to the inner mitochondrial membrane by the steroidogenic acute regulatory (StAR) protein; the conversion from cholesterol to pregnenolone -catalyzed by the cholesterol side chain-cleaving enzyme (the gene product of CYP11A1)- takes place. Pregnenolone then exits the mitochondria and is converted to progesterone by the 3β-hydroxysteroid dehydrogenase (3β-HSD mainly isoform II in humans and isoforms I and VI in mice (11; 12)) in the endoplasmic reticulum. Progesterone is then further hydroxylated in the position 21 to form 11-deoxycorticosterone, a step catalyzed by the gene product of CYP21A. The aldosterone synthase (CYP11B2), at the matrix side of the inner mitochondrial membrane, catalyzes the hydroxylation and 18 oxidation of 11-deoxicorticosterone, yielding aldosterone.

Aldosterone biosynthesis can be divided into two phases depending on the temporal distance to the stimulus. Thus, acute regulation (minutes to hours after the stimulus) relies on the movement of cholesterol into the mitochondria mediated by the increased activity and expression of StAR, and probably also by upregulation of aldosterone synthase levels (13). On the other hand, during chronic stimulation (hours to days) aldosterone production is primarily controlled by the expression of the aldosterone synthase.

1.2 Role of aldosterone in the regulation of blood pressure and extracellular fluid balance

In the kidney, aldosterone is crucial for Na^+ and K^+ homeostasis by acting on the principal and intercalated cells of the aldosterone-sensitive distal nephron (which comprises the distal convoluted tubule, the connecting tubule and the cortical collecting duct). Aldosterone stimulates transepithelial Na^+ transport together with K^+ excretion in the kidney by mechanisms such as:

- Transcriptional upregulation and post-transcriptional activation of the amiloride sensitive epithelial Na^+ channel (ENaC) in the apical membrane (14-16).
- Induction of the basolateral Na^+/K^+-ATPase activity (17; 18).
- Plasma membrane expression of KCNJ1 (ROMK) K^+ channels in the apical membrane (19; 20).
- Activation of Na^+/H^+ exchanger in the basolateral membrane (21).

The movement of electrolytes from the lumen of the tubular system into the extracellular compartment is accompanied by water, so as to maintain the osmotic balance. Therefore, aldosterone regulation of salt and water homeostasis ultimately also regulates plasma volume and consequently blood pressure.

Actions of aldosterone can be classified as genomic (of major importance) or non-genomic (of minor importance), depending on the receptor and the signal transduction mechanism involved. The genomic action is mediated by the binding of the hormone to the mineralocorticoid receptor (MR) located in the cytosol. Non-genomic actions seem to be mediated both by the MR and probably by a plasma membrane-associated receptor (15; 16; 22).

Most of the genomic actions of aldosterone on epithelial cells are mediated by the serum and glucocorticoid inducible kinase isoform 1 (SGK1) (14; 23; 24). Non-genomic effects appear to be mediated by second messengers such as cyclic adenosine monophosphate (cAMP), intracellular Ca^{2+} concentrations ($[Ca^{2+}]_i$) and inositol 1,4,5-trisphosphate (IP_3) production (22; 25-27). The participation and modulation of protein kinases is also common in these pathways (27-30).

Figure 1.3 summarizes the effects of aldosterone in the aldosterone-sensitive distal nephron.

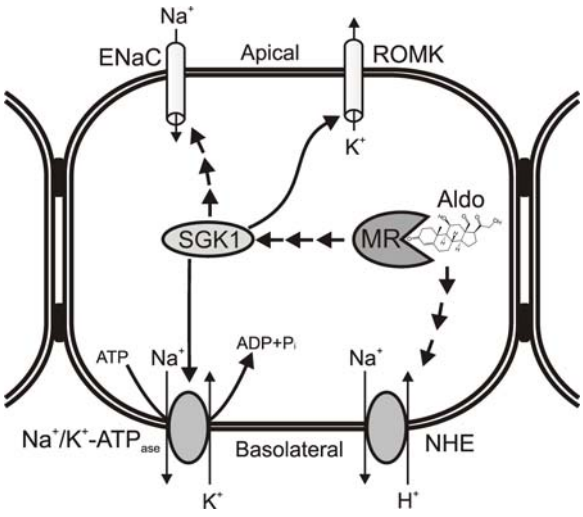

Figure 1.3. Simplified scheme of the effects of aldosterone in the aldosterone-sensitive distal nephron involved in Na^+ reabsorption and K^+ excretion. Acronyms are: MR. Mineralocorticod receptor; Aldo. aldosterone; NHE. Na^+/H^+ exchanger; SGK1. Serum and Glucocorticoid inducible Kinase isoform 1; ENaC. Epithelial Na^+ channel; ROMK. Renal outer medullary K^+ channel (KCNJ1). Action of aldosterone on the NHE seems to be mediated by PKC and independent from SGK1 (21; 31; 32). Apical expression of the large conductance Ca^{2+} activated K^+ channel (MaxiK) is also increased in the cortical collecting duct of animals subjected to a rich K^+ diet (30). However, it seems that aldosterone is not directly involved in this mechanism (33).

Recently a novel type of kinases named “with no Lysine” (WNK) has shed light on many actions of aldosterone in the aldosterone-sensitive distal nephron. Hence, WNKs have been found to be involved in the regulation of ROMK, ENaC, the $Na^+/K^+/2Cl^-$ cotransporter isoform 2 (NKCC2), and Na^+/Cl^- cotransporter (NCC) (34-37).

Besides its action on the kidney and the regulation of plasma volume, aldosterone also targets other organs involved in the regulation of blood pressure. For instance, in the vascular system, aldosterone produces vasoconstriction and promotes endothelial cell stiffness (38; 39) while in the central nervous system it regulates blood pressure probably via changes in salt appetite (15; 40; 41). Aldosterone has also been found to participate in the hypertension-related remodeling of the heart, promoting vascular and myocardial fibrosis (42; 43).

1.3 Regulation of aldosterone secretion

Due to its importance in the maintenance of blood pressure and fluid balance, it is not surprising that aldosterone secretion is tightly controlled by several factors and involves various cellular pathways. Many factors have been described to modulate aldosterone

secretion in glomerulosa cells (44). The most relevant are angiotensin II, hyperkalemia and ACTH as stimuli and atrial natriuretic peptide (ANP) as an inhibitor.

1.3.1 The Renin-Angiotensin System (RAS)

Renin is an aspartyl-protease produced as an enzymatically inactive precursor in the juxtaglomerular cells of the afferent arterioles of the kidney. Various events such as the reduction of extracellular fluid volume, the fall of renal perfusion pressure, the acute activation of sympathetic outflow to the kidney, the release of catecholamines and Na^+ deficiency may induce the release of renin, which is in turn the rate limiting step of the activation of the RAS. Once renin has been released and activated, it cleaves angiotensinogen (constitutively produced by the liver) and releases the decapeptide angiotensin I (AngI). AngI is then further modified by the carboxypeptidase angiotensin converting enzyme (ACE) to produce the octapeptide AngII - the physiologically active component of the system. Further cleavage of AngII by aminopeptidases A and N produces AngIII (Ang 2-8) and AngIV (Ang 3-8). AngII also controls its own production by inhibiting the production of renin on the juxtaglomerular cells, thus creating a negative feedback loop (Figure 1.4).

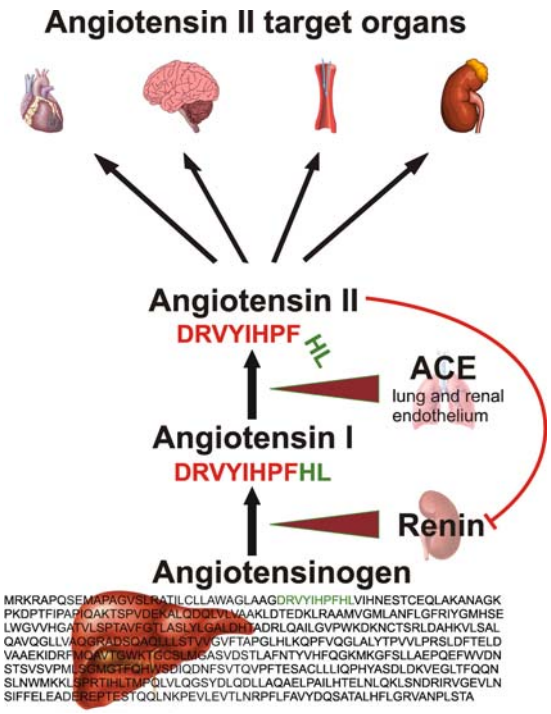

Figure 1.4. Overview of the renin-angiotensin system. For further details see text.

AngII further exerts its action by binding to AngII receptors (AT) 1 and 2, members of the large family of G-coupled seven-transmembrane spanning receptors. Most of the classical actions of AngII related to cardiovascular effects are elicited by its specific binding to the AT1 receptor (45-47). Among others, these include:

- Intense vasoconstriction (48),
- Stimulation of adrenal aldosterone secretion (13; 44; 49-55), (see section 1.3.2),
- Ionotropic and chronotropic effects on cardyomyocytes (56),
- Release of catecholamines from the adrenal medulla (57),
- Modulation of drinking behavior and salt appetite (58),
- Na^+ reabsorption (46),
- Cell proliferation (59),

Interestingly, both renin expression and AngII secretion also occur in glomerulosa cells of the adrenal gland, 20-25% of which release AngII (44). Chromaffin cells distributed throughout the whole cortex have been described to express renin and to present AngII secretory granules. (44) This intra-adrenal RAS has been suggested to amplify the effect of the systemic RAS.

Most of all, increase of aldosterone secretion may be attributed to the increased activity of the RAS and/or increased plasma levels of K^+. However, under conditions of severe loss of Na^+ or fluid, ACTH is also secreted and synergizes with AngII or K^+ in the stimulation of glomerulosa cells. On the other hand, ANP secretion is increased in response to Na^+ and/or water loading and inhibits aldosterone production.

1.3.2 Cytoplasmic Ca^{2+} signal triggered by AngII in glomerulosa cells

In *zona glomerulosa* cells, AngII binds to the AT1 subtype receptors present in the plasma membrane (60). The subtype q of the heterotrimeric G protein (G_q) coupled to AT1 mediates the activation of phospholipase C (PLC) (61). PLC is also activated by

high $[Ca^{2+}]_i$ (62), and its enzymatic activity yields inositol 1,4,5-trisphosphate (IP_3) and diacylglycerol (DAG). IP_3 then binds to the IP_3 gated Ca^{2+} channels in the endoplasmic reticulum (ER), thus allowing the release of Ca^{2+} to the cytoplasm. This Ca^{2+} signal is concentration dependent and ranges from an oscillatory activity upon application of pM concentrations of AngII to a typical peak-plateau pattern in response to nM concentrations of the agonist (63).

A sustained cytoplasmic Ca^{2+} signaling is achieved in part due to the store release of this divalent cation, as well as its influx from the extracellular compartment. Binding of AngII to the AT1 receptor depolarizes glomerulosa cells and therefore activates the T-type voltage-sensitive Ca^{2+} channels present in the plasma membrane (64). As a result, Ca^{2+} enters the cell where the concentrations are 10 000 times lower compared to the extracellular compartment. It is clear then that the maintenance of the membrane voltage (V_m) is a crucial step for the cytoplasmic Ca^{2+} signaling triggered by AngII. Under basal conditions, the V_m of glomerulosa cells is close to that predicted by the Nernst equation for a cell which is only permeable to K^+ (65; 66), thus the voltage activated Ca^{2+} channels are inactive. This strikingly high K^+ conductance is only possible due to the presence of two-pore domains “leakage” K^+ (K_2P) channels Task1 (KCNK3), Task3 (KCNK9) and Trek1 (KCNK2) (65; 67-70). The reduction of the permeability to K^+ would shift the membrane voltage from the very negative values close to the K^+ equilibrium potential (-90mV) towards the more positive equilibrium potentials of Ca^{2+} and Na^+ (123 mV and 67 mV, respectively). The depolarization triggered by AngII is achieved by the inhibition of K^+ leakage channels. The precise molecular mechanism of this inhibition is still controversially discussed (68; 70-72).

It has been also shown that AngII augments T-type Ca^{2+} currents in a GTP-dependent manner in bovine glomerulosa cells (73). Although L-type Ca^{2+} channels are also expressed in *zona glomerulosa* cells; several evidences suggested an inhibition of these channels by physiological concentrations of AngII (74-76).

The third major action of AngII on increasing $[Ca^{2+}]_i$ is its effect on the store-operated Ca^{2+} influx. Ca^{2+} store depletion in rat and bovine glomerulosa cells promotes aldosterone production (77; 78). The family of the transient receptor potential proteins (Trp) has also been proposed to be involved in this mechanism (79-81). Both the mRNA and protein products of Trp 4 have been detected in the adrenal cortex (82). However, further studies are needed in this field since there are no reports in

glomerulosa cells regarding the recently discovered constituents of the store operated calcium influx: the ER Ca^{2+} sensor stromal interaction molecules (STIM); and the plasma membrane channels Orai (83).

1.3.3 Cytoplasmic Ca^{2+} signal triggered by hyperkalemia in glomerulosa cells

As mentioned before, glomerulosa cells are hyperpolarized under basal conditions due to the presence of K_2P leakage channels, which provide them with a unique K^+ sensitivity (67). Changes in extracellular K^+ concentrations ($[K^+]_o$) will thus shift the resting membrane voltage to more positive values (depolarizing the cell) when $[K^+]_o$ increases, or hyperpolarizing the cell when it decreases.

Hyperkalemia, one of the strongest secretagogues of aldosterone, depolarizes glomerulosa cells, which in turn activates the T-type voltage gated Ca^{2+} channels and increases $[Ca^{2+}]_i$. This effect of K^+ upon Ca^{2+} is nonoscillating and long lasting (44). Under supraphysiological $[K^+]_o$ concentrations, L-type Ca^{2+} channels can also be activated (64; 84).

1.3.4 Regulation of $[Ca^{2+}]_i$ increase

$[Ca^{2+}]_i$ increase elicited by aldosterone secretagogues must be regulated in order to prevent overreaction of the stimulated cell and to prepare it for consequent stimulations. $[Ca^{2+}]_i$ can be regulated through several mechanisms:

- Inhibition of L-type voltage gated Ca^{2+} channels by Ang II in order to prevent Ca^{2+} overloading (75).
- The plasma membrane Ca^{2+} ATPase (PMCA) and the SERCA remove Ca^{2+} by transporting it actively either to the extracellular compartment or into the endoplasmic reticulum respectively.
- The Na^+/Ca^{2+} antiporter present in the plasma membrane exchanges three Na^+ for one Ca^{2+} allowing net Ca^{2+} efflux.

1.3.5 Integration of the intracellular pathways controlling the synthesis of aldosterone

The signaling pathways involved in $[Ca^{2+}]_i$ increase upon stimulation by AngII and hyperkalemia are summarized in Figure 1.5.

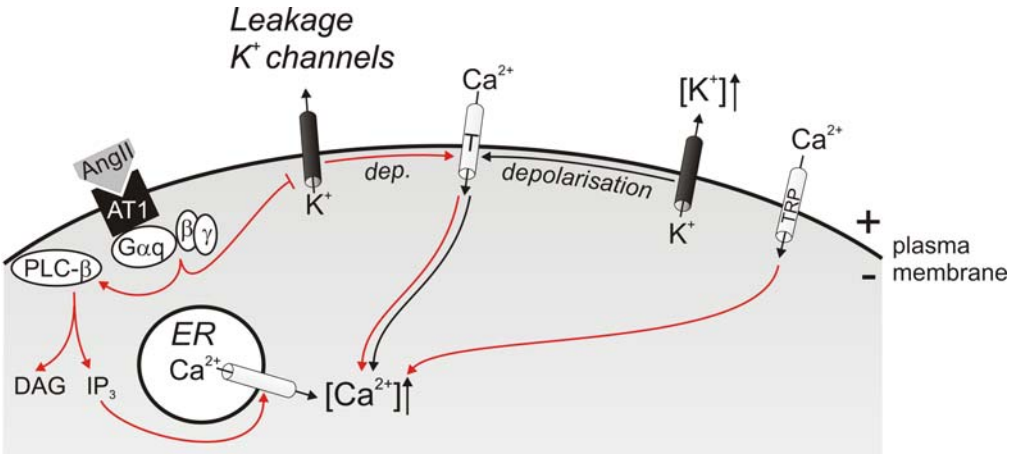

Figure 1.5. Schematic representation of cytoplasmic Ca^{2+} increase elicited by AngII (red arrows) and hyperkalemia (black arrows). Acronyms used are: AngII, angiotensin II; AT1, AT1 type receptor of angiotensin II; Gαq, alfa subunit of the heterotrimeric G protein subtype q. β and γ represent the other two subunits; PLC-β, beta-subunit of the phospholipase C enzyme; DAG, diacylglycerol; IP_3, inositol 1,4,5-trisphosphate; ER, Endoplasmic reticulum; T, T-type voltage gated Ca^{2+} channels; TRP, transient receptor potential protein 4. Adapted from Bandulik, S. *et al*., 2010 (85).

A cascade of events is triggered upon $[Ca^{2+}]_i$ increase. This includes the activation of protein kinase C (PKC) as well as the mitogen-activated protein kinases (MAPKs) ERK1 and ERK2, ultimately resulting in the expression of StAR (13; 86). In turn, the activation of these MAPKs depresses DAX-1, a transcription factor known to inhibit the SF-1 dependent transcription of StAR. The activity of StAR also requires phosphorylation which can be accomplished either by protein kinase A (PKA) (activated during ACTH stimulation of steroidogenesis) or by PKC (87).

Increased $[Ca^{2+}]_i$ is also followed by the activation of the Ca^{2+} binding protein calmodulin (CaM) which then activates CaM kinases (CaMKs) I and/or IV (13; 88). The phosphorylation of the transcription factors ATF-1, Nurr1 and CREB by CaMKs induces the activation of the CYP11B2 promoter (13).

The activation of CaMKII in bovine glomerulosa cells has been associated with a reduction of the activation threshold of T-type voltage activated Ca^{2+} channels (89). This mechanism serves as positive feedback and could be involved in the amplification of the signal generated after small changes of $[K^+]_o$.

1.4 Potassium channels and their function in the adrenal gland

Potassium channels are components of a diverse and ubiquitous family of membrane proteins present in both excitable and non-excitable cells. Members of this superfamily play critical roles in cellular signaling processes such as regulating neurotransmitter release, heart rate, hormone secretion, neuronal excitability, epithelial electrolyte transport, smooth muscle contraction and cell volume regulation (90). A large number of genetic mutations in K^+ channels linked to human diseases have been described in the past years, highlighting the importance of these molecular entities.(91-94)

Until now 78 pore-forming K^+ subunits have been described in humans (for detailed information and further links refer to: http://www.genenames.org/genefamily/kcn.php) comprising four major K^+ channels subfamilies namely: voltage-gated, inwardly rectifying, calcium dependent and two pore domains K^+ channels (95).

Recently, an exhaustive list of the expression of K^+ channels in the human adrenal cortex has been published (91). Moreover, some of them have been found to be related to pathological conditions in both animal models and humans (Table 1.1).

Table 1.1. Expression of potassium channels in the adrenal glands[a]. Modified from Bandulik, S. *et al*., 2010 (85).

Channel	Adrenal expression	Species	Function	Pathophysiology	Ref.
Task1 (*KCNK3*)	ZG > ZF > ZR; (mouse). EST, PCR, in situ hybridization, Human Gene 1.0 ST array	Rat mouse Human	Resting membrane potential, part of acid- and AngII-sensitive current	Altered expression pattern of aldosterone synthase, hyperaldosteronism (sex-dependent) in Task1$^{-/-}$ mice	(65; 66; 70; 91)
Task2 *(KCNK5)*	ZR (own unpublished data). PCR, Human Gene 1.0 ST array	Mouse Human	Unknown	Unknown	(68; 91)
Task3 *(KCNK9)*	ZG specific expression. PCR, in situ hybridization, Human Gene 1.0 ST array	Rat mouse Human	Probably heterodimers with Task1, resting membrane potential	Primary hyperaldosteronism in adult male Task1$^{-/-}$/Task3$^{-/-}$ mice	(65; 68; 91; 96; 97)
Task4 *(KCNK17)*	Cloned from adrenal cDNA, Human Gene 1.0 ST array	Human	Unknown	Unknown	(91; 98)
Task5 *(KCNK15)*	Northernblot, PCR, Human Gene 1.0 ST array	Human	Unknown	Unknown, inactive, cytosolic Expression	(91; 99)
Trek1 *(KCNK2)*	Adrenal cortex (in situ hybridization, PCR), ESTs, Human Gene 1.0 ST array	Bovine human Mouse	Inhibition of Trek1 current by Ang II and ACTH, induced expression by ACTH	Unknown	(91; 100-104)
KvLQT1 / IsK (*KCNQ1 / KCNE1*)	PCR, EST, Human Gene 1.0 ST array	Mouse Human	Repolarization of membrane potential	Increased aldosterone secretion under hyperkalemia in KCNE1$^{-/-}$ mice	(91; 105; 106)
MaxiK (*KCNMA1 / KCNMB1*)	PCR, ESTs, Human Gene 1.0 ST array	Mouse Human	K^+ conductance stimulated by ANP leading to reduced aldosterone secretion	Hyperaldosteronism in KCNMA1$^{-/-}$ mice. Controversial phenotype of KCNMB1$^{-/-}$ mice	(84; 91; 107; 108)
Kir3.4 (*KCNJ5*)	ZG specific expression (Immunohistochemistry), ESTs, Human Gene 1.0 ST array	Human	Functional relevance is controversial	Mutations found in APAs and familial non-glucocorticoid-remediable aldosteronism.	(91; 109-111)

[a] The " KCN " nomenclature of the " Human Genome Organisation " (HUGO; http://www.genenames.org/genefamily/kcn.php) is shown in parentheses. ZG: zona glomerulosa; ZF: zona fasciculata; ZR: zona reticularis; EST: expressed sequence tags (http://www.ncbi.nlm.nih.gov/sites/entrez?db=unigene)

1.5 K_2P channels

In 1996 Lesage and co-workers cloned and described the first member of the mammalian K_2P potassium channel subfamily called TWIK (tandem of pore domains in a weak inwardly rectifying K^+ channel, now called TWIK-1) (112). Until now 15 members of the K_2P family have been described and subdivided into 6 subfamilies (TWIK, TREK, TASK, TALK, THIK and TRESK) on the basis of sequence similarity and

functional resemblance (Figure 1.6. A). As indicated by their name, the characteristic molecular topology of the K_2P channels is the presence of two pore forming domains per molecule (Figure 1.6. B), in contrast to the other K^+ channel families characterized by one pore forming domain per subunit (113). K_2P subunits dimerize to constitute the functional K^+ selectivity filter containing four pore loop domains, a structure characteristic of all known K^+ channels.

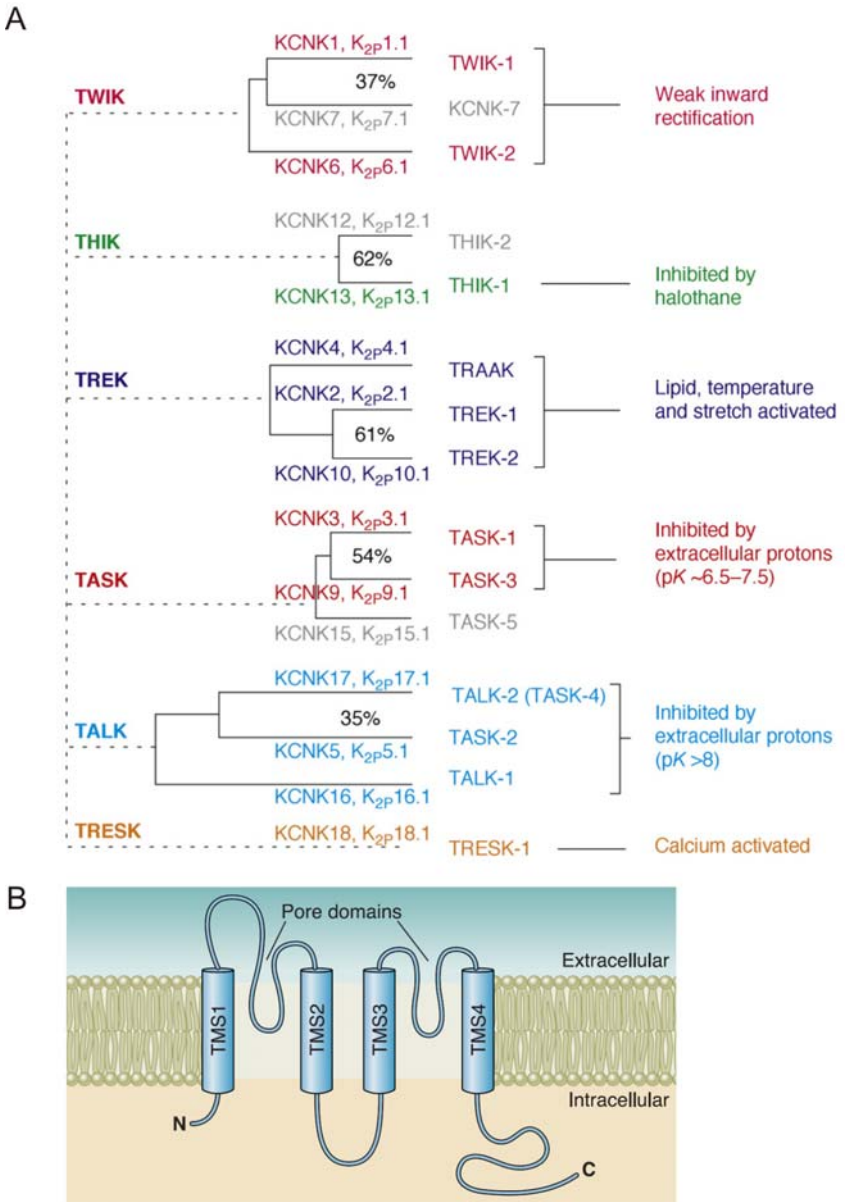

Figure 1.6. **A.** Phylogenetic tree of the known members of the human K_2P family classified into 6 subfamilies. The genes that have not produced functional channels are shown in grey. Both the conventional (TWIK, tandem of P domains in a weak inwardly rectifying K^+ channel; THIK,

tandem pore domains halothane-inhibited K^+ channel; TREK, TWIK related K^+ channel; TRAAK, TWIK-related arachidonic acid-stimulated K^+ channel; TASK, TWIK-related acid-stimulated K^+ channel; TALK, TWIK-related alkaline pH activated K^+ channel; TRESK TWIK-related spinal cord K^+ channel) and the systematic (The Human Genome Organization (HUGO) uses KCNK designation and The International Union of Pharmacology (IUP) replaces the KCNK by a K_{2P} prefix) names are indicated. Reproduced from Bayliss, D.A. and Barret, P.Q. 2008 (113) **B**: Schematic transmembrane topology of human K_2P channels. TMS: transmembrane segment. Reproduced from Enyedi, P. and Czirják, G. 2010 (95).

K_2P channels are widely expressed in human tissues (114) where they give rise to background K^+ currents (95; 113). They exhibit very weak voltage dependence and a weakly rectifying current-voltage relationship, remaining open at negative membrane potentials (95). In addition, K_2P channels are regulated by a variety of physicochemical factors, endogenous neurochemicals, signaling pathways and clinically relevant drugs. It is thus not surprising that differential expression of K_2P subunits can provide cells with a rich modulatory potential (95).

The K_2P channel Trek1 has been identified as a key factor in the regulation of aldosterone and cortisol secretion in bovine adrenal cortex and in the human cell line NCI H295R (69). It is thought to be one of the major K^+ channels controlling the membrane potential in *zona glomerulosa* and *zona fasciculata* bovine cells -where Trek1 currents are inhibited by ACTH and AngII- (100; 101; 115). Although Trek1 is highly expressed in both human (91), and mouse adrenal cortex (85), up to now its relevance for the adrenal gland function in these two species has not yet been investigated at a functional level. As pointed out previously, there are important differences regarding the production of steroids among different species: **i)** in bovine (as well as in swine) cells, the synthesis of aldosterone and cortisol is carried out by only one enzyme (116), whereas in rodents and humans two different enzymes take part in this functions; **ii)** Task channels dominate the potassium conductance of glomerulosa cells of mice (65; 66) and rats (68), where Trek channels appear to be less important.

1.5.1 Task channels

The Task group comprises the acid pH sensitive members of the K_2P channels family Task1, Task3 and Task5. Although Task5 cannot be functionally expressed, it was classified into the Task group based in the amino acid (aa) sequence similarity.

Task1 gene is located at position 2p23 of the human chromosome 2 and encodes a 43.5 kDa protein with 394 aa. On the other hand, Task3 is located at position 8q24.3 of the human chromosome 8 and encodes a 42.3 kDa protein with 372 aa. In mouse Task1 and Task3 genes are located on chromosomes 5 and 15 respectively and encode slightly larger proteins with 409 aa (45 kDa) and 402 aa (44.9 kDa), respectively.

Task1 and Task3 exhibit a high sequence similarity (see Figure 1.6. A) and therefore are closely related at the molecular level: they are both extremely sensitive to variations of extracellular pH in the physiological range (Task1 is more sensitive in the physiological pH range than Task3), inhibited by acidification (97; 117-119) and activated by the volatile anaesthetics halothane and isoflurane (120; 121). Moreover, Task1 and Task3 are the only subunits among the K_2P family that have been reported to form heterodimers *in vitro* (97) and *in vivo* (122). On the other hand, Task3 is selectively inhibited by Zn^{2+} (123) and is the only member of the K_2P channels that is genetically imprinted in humans and mouse; i.e. the maternal allele is preferentially expressed (124-126).

In addition to the central nervous system, the adrenal cortex is a primary site of Task channels expression (113). In mice Task1 is expressed in *zona glomerulosa* and *zona fasciculata* cells whereas Task3 mRNA has been found to be predominantly expressed in *zona glomerulosa* cells (65; 66; 85).

1.5.2 The adrenal phenotype of Task1$^{-/-}$ and Task1$^{-/-}$/Task3$^{-/-}$ mouse models

Knockout animal models have been widely used to study the contribution of given genes to a particular physiological process. In the last years the importance of Task channels for aldosterone secretion *in vivo* has been addressed using such models (65; 66; 85; 127).

In 2008 Heitzmann and co-workers (66) reported a severe adrenal phenotype in adult Task1$^{-/-}$ animals. Surprisingly, only female knockout animals exhibited a striking hyperaldosteronism linked to hypertension, while male animals showed no adrenal phenotype. The hyperaldosteronism was independent of Na^+ and K^+ intake and appeared despite the hypokalemia and low plasma renin activity present in female knockouts, and was therefore considered as primary hyperaldosteronism. An analysis of the localization of aldosterone synthase within the adrenal cortex revealed that this loss of the physiological control of the aldosterone secretion was due to an ectopic localization of this enzyme. In female knockout animals, aldosterone synthase was expressed in *zona fasciculata* cells instead of the normal glomerulosa localization (Figure 1.7). Remarkably, the hyperaldosteronism was remediable by treating the animals with the synthetic glucocorticoid dexamethasone, pointing to an ACTH-dependent regulation of aldosterone secretion in these mice. In this regard, these mice could provide a model of the glucocorticoid remediable hyperaldosteronism also present in humans. However, the problem underlying this disease is different in most of the patients, where an unequal crossing over between the CYP11B1 (coding the 11β-hydroxylase enzyme, responsible for the production of cortisol) and CYP11B2 genes is causative for this disorder. The genes of CYP11B1 and CYP11B2 are 95% identical and in close proximity in chromosome 8. Thus, in the human glucocorticoid remediable hyperaldosteronism, the 5' regulatory region of the CYP11B1 gene is fused to the coding region of CYP11B2 and therefore the transcription of the CYP11B2 gene is now controlled by ACTH (128).

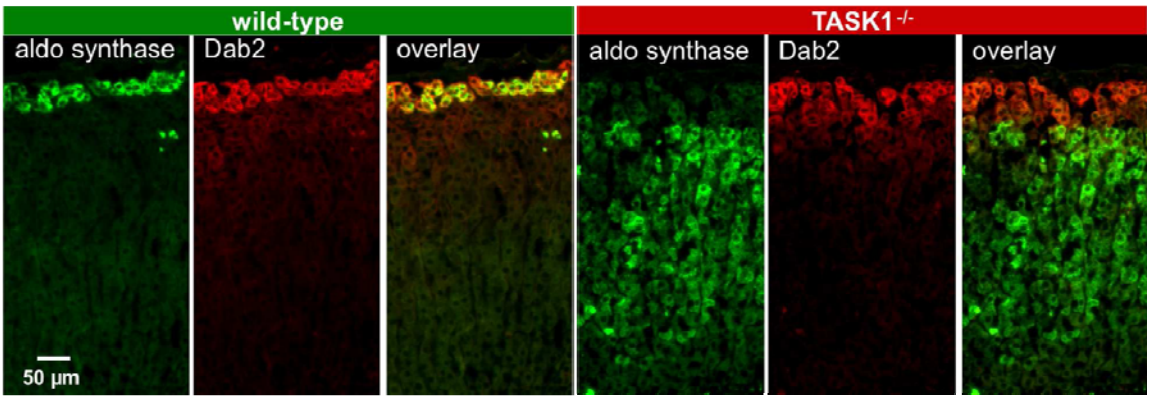

Figure 1.7. Effect of Task1 invalidation on adrenocortical zonation. Immunofluorescence of: aldosterone synthase (green) and the *zona glomerulosa* specific marker Disabled-2 (Dab2), red) (129). Left panel: adrenal cortex of a female wild type mouse; right panel: adrenal cortex of a female Task1$^{-/-}$ mouse. Adapted from Bandulik, S. *et al*., 2010. (85).

A more recent paper (85) provided additional evidences indicating that the abnormal zonation of Task1$^{-/-}$ mice was due to an ectopic expression of aldosterone synthase rather than to wrongly localized glomerulosa cells. As presented in Figure 1.7, *zona glomerulosa* cells expressing the specific marker Dab2 did not express aldosterone synthase. These data suggests that regulatory mechanisms controlling aldosterone secretion in Task1$^{-/-}$ glomerulosa cells are still preserved. The elevated plasma aldosterone concentration induces a negative feedback in glomerulosa cells where aldosterone production is switched off.

The invalidation of the Task1 channel also highlighted its importance for the development of the adrenal cortex and the dynamics of adrenocortical zonation. Heitzmann and co-workers observed that aldosterone synthase in both, female and male Task1$^{-/-}$ mice, was abnormally localized before puberty, and became normal only in adult male mice. Gender and age differences in the adrenocortical zonation of aldosterone synthase raised the question whether sex hormones regulate the underlying compensatory mechanisms in adult male animals. Indeed, aldosterone synthase dezonation could be recapitulated in castrated male mice. Moreover, it was also possible to recover the normal zonation pattern in female mice after testosterone treatment.

Regarding the electrophysiological properties of adrenocortical primary cells, Task1$^{-/-}$ cells were depolarized by about 7 mV under control conditions when compared to Task1$^{+/+}$ cells. However, upon addition of AngII or after extracellular acidification the cells further depolarized, indicating the presence of other acid sensitive K^+ channel, possibly Task3 homodimers.

This work clearly demonstrated the crucial importance of Task1 K^+ channels in the regulation of zonation and biochemical properties of the adrenal cortex. However, the nature of other channels or factors (under the transcriptional control of testosterone), underlying the compensatory mechanism in male Task1$^{-/-}$is still unknown.

Another milestone for the understanding of the role of K_2P channels for aldosterone secretion in mice was published by Davies and co-workers only few months later (65), on Task1$^{-/-}$/Task3$^{-/-}$ double knockout mice. Surprisingly aldosterone synthase appeared to be normally localized in adult males Task1$^{-/-}$/Task3$^{-/-}$, while females were not included in this study.

Using freshly prepared adrenal slices for patch clamp measurements, the authors observed that *zona glomerulosa* cells from Task1$^{-/-}$/Task3$^{-/-}$ mice were depolarized by about 20 mV. This result, together with the absence of pH inhibitable and halothane activatable K^+ currents unequivocally led to the conclusion that Task1 and Task3 channels conduct a background K^+ current in *zona glomerulosa* cells.

Similarly to Task1$^{-/-}$ female mice, increased production of aldosterone was observed in male Task1$^{-/-}$/Task3$^{-/-}$ when compared to wild type animals and despite the low plasma concentrations of renin. This phenotype was independent of the salt intake and therefore classified as primary hyperaldosteronism. As expected, these mice were also hypertensive. Interestingly, the production of aldosterone in Task1$^{-/-}$/Task3$^{-/-}$ mice was increased by low Na^+ diet and reduced by the administration of the AT1 receptor blocker candesartan. Nevertheless aldosterone levels remained higher than in wild type mice. Altogether these results suggest that in mice lacking both, Task1 and Task3 K^+ channels, aldosterone levels are still under the regulation of AngII, at least to some extent.

2 Objectives

Although in recent years our comprehension of the molecular mechanisms involved in the regulation of aldosterone secretion has improved, we are still far from thoroughly understanding this important physiological process. The control of the membrane voltage in aldosterone producing cells by K_2P channels has been identified as a pivotal factor in this complex scenario. Therefore, the present work was aimed at investigating the particular contribution of the K_2P channel Task3 to the regulation of aldosterone secretion.

Towards this general goal the following specific objectives were postulated:

1. To investigate the expression and localization of Task3 in the mouse adrenal gland.

2. To evaluate the contribution of Task3 to the K^+ sensibility of adrenocortical cells and tissues.

3. To study the impact of the deletion of Task3 on the response of adrenocortical cells and tissues to angiotensin II.

4. To investigate the impact of the deletion of Task3 on the regulation of the aldosterone secretion *in vivo*.

3. Materials and Methods

3 Materials and Methods

All the reagents were purchased from Sigma, (Taufkirchen, Germany) or Merck (Darmstadt, Germany) unless otherwise stated.

3.1 Mice

3.1.1 The Task3$^{-/-}$ knockout mouse model

The Task3$^{-/-}$ knockout mouse was generated by Guyon and co-workers as described previously (130). The following description was modified from their published study: briefly, the Task3 gene locus was targeted for homologous recombination in 129/Sv embryonic stem cells. The vector was designed to allow cre-mediated deletion (131) of exon 2, which encodes pore domains P1 and P2, the transmembrane domains M2-M4 as well as the cytoplasmic C-term of Task3 (for details refer to Figure 1.6 B). Primers were designed to amplify three contiguous DNA fragments of 6.6 kb (long arm), 1 kb (containing exon 2), and 2.9 kb (short arm) from 129/Sv genomic DNA (Figure 3.1)

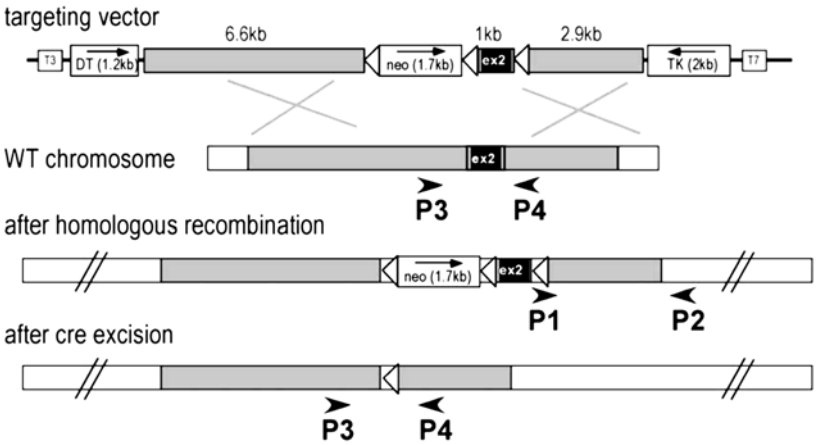

Figure 3.1. Schematic strategy of inactivation of Task3 gene. Open triangles represent loxP sequences. For further details see text. Reproduced from Guyon, A. *et al.*, 2009 (130).

PCR products were subcloned into a modified pBluescript (Stratagene) containing a neomycin (neo) resistance cassette for positive selection, as well as thymidine kinase (TK) and diphtheria toxin (DT) genes to select against random incorporations. LoxP sites were added flanking the second exon and the neomycin resistance cassette for further gene inactivation by excision using the cre recombinase. After linearization, the targeting vector

was transfected by electroporation into embryonic stem (ES) cells by Genoway Company. DNA extracted from colonies resistant to the antibiotic G418 (resistance conferred by the neo gene) was analyzed by PCR using a 5` primer overlapping the sequence junction between the loxP sequence and the 5` end of the short arm and a 3' primer external to the targeted sequence. A positive clone was further characterized by Southern blot analysis using probes corresponding to 5' and 3' sequences flanking the targeted regions to ensure integrity of the targeted locus. Genoway Company also performed blastocyst injection. Chimeric animals were identified by coat color and crossed to C57BL/6J mice. Tail DNA was analyzed by PCR to select progeny bearing the floxed allele, which was then crossed to a mouse strain expressing the cre-recombinase under the cytomegalovirus promoter (CMV-cre). Exon 2 excision in offspring was assessed by PCR using primers flanking this region

Task3$^{-/-}$ mice were backcrossed for at least 10 generations into the C57Bl/6 genetic background. All the mice used in this work were aged between 12 and 48 weeks (unless otherwise mentioned) and age matched for each experiment. Wild type mice (hereafter designated Task3$^{+/+}$) were from the C57BL/6 inbreed strain (The Jackson Laboratory, Maine, USA).

3.1.2 General animal keeping and experimental conditions

Animals were maintained on a normal diet (chow, R03T-25; SAFE, 0.75% K^+, 0.27% Na^+) with free access to food and water. The experimental protocols were approved by the local councils for animal care and were conducted according to the German and French law for animal care.

For the experiments mice were fed with high (3%) or low (<0.05%) K^+ diet (INRA, France or Ssniff Spezialdiäten GmbH, Soest, Germany). Alternatively, high K^+ diet was attempted by adding 200 mM KCl and 12% sucrose in the drinking water. Rich (4% NaCl) or low (<0.03% NaCl) Na^+ diets (Ssniff Spezialdiäten GmbH, Soest, Germany) were also used. For all protocols, animals were subjected to the special diet condition for at least 1 week before the measurements.

Mouse anaesthesia was carried as follows; animals were subject to 2.5-3 % (Task3$^{-/-}$ animals display reduced sensitivity to volatile anaesthetics) of isoflurane (Baxter Deutschland GmbH, Unterschleißheim, Germany) administered with a vaporizer (MFI Föhr

Medical Instruments GmbH, Seeheim, Germany) in a mixture of 50% oxygen and 50% nitrogen.

3.1.3 Hormonal treatment and castration

Five weeks old Task3$^{+/+}$ male mice were anesthetized as described in section 3.1.2 and castrated via scrotal incision. Five weeks after castration, mice were injected once a day during 6 days with 1 µg of testosterone propionate (Sigma-Aldrich, Steinheim, Germany) per g of body weight at the beginning of the treatment. Testosterone was administered subcutaneously, dissolved in sesame oil (0.5 mg/mL). Mice included in the vehicle treated group were injected with an equivalent volume of sesame oil.

Prior to adrenal glands fixation by perfusion for immunofluorescence (see section 3.3), the left renal artery and vein were clamped and the left adrenal gland was removed for cDNA preparation and real time-PCR.

Female mice followed the same treatment as castrated male mice.

3.2 Blood analysis

Blood was collected into heparin-treated capillary tubes from facial vein after lancet prick. Alternatively blood was collected from the orbital sinus from previously anesthetized mice. Samples were centrifuged and plasma was frozen and kept at -20°C.

3.2.1 Aldosterone measurements

Aldosterone was measured either by using a solid-phase ^{125}I Radioimmunoassay (RIA) kit (Immunotech, Marseille, France) or enzyme-linked immunosorbent assay (ELISA) kit (Diagnostic Biochem Canada Inc, Ontario, Canada) according to manufacturer instructions. Both methods exhibit low cross reactivity to other endogenous steroids.

3.2.2 Plasma renin activity (PRA)

For the measurement of the PRA, blood samples were taken from a facial vein and incubated for 1.5 h at 37°C with plasma of bilaterally nephrectomized male rats as renin substrate. The production of AngI (ng/ml/h) was measured by ^{125}I RIA (Byk and DiaSorin Diagnostics, Germany) to determine the PRA.

3.3 Immunofluorescence

After incision of the *vena cava inferior*, anesthetized mice were sacrificed by removal of the blood by perfusion with 10 ml of 0.9% NaCl solution supplemented with 10 IU/ml of heparin (Heparin-Natrium-25000, Ratiopharm GmbH, Ulm, Germany). Next, mice were perfused with 45 ml of fixation solution I (EGTA 1 mM; K_2HPO_4 15 mM; $MgCl_2$ 2 mM; NaCl 90 mM; Paraformaldehyde (PFA) 3%; Sucrose 100 mM, pH 7.4). All the solutions were administered through a polyethylene catheter inserted into the abdominal aorta, at a constant flow rate of 10 ml/min assured with a roller pump (Ismatec SA, Glattbrugg, Switzerland). Adrenal glands were then harvested, and placed in chilled fixation solution II (the same composition as fixation solution I but with 17% Sucrose and 1% PFA instead). After 30 min of incubation, adrenals were frozen into -40°C cold methyl butane and kept at -80°C until further handling.

Adrenals were embedded in Optimal Cutting Temperature (OCT)-Compound (Sakura Finetek Germany GmbH, Staufen, Germany) and sliced into 5 µm thick sections using a Cryostat CM3050 S (Leica, Wetzlar, Germany). Sections were placed on Poly-lysine slides (Kindler, Freiburg, Germany). For unmasking of epitopes, the sections were incubated in 0.1% SDS dissolved in PBS (KH_2PO_4 1.8 mM; Na_2HPO_4 10.3 mM; NaCl 137 mM; pH 7.4) for 5 min. After washing with PBS, the samples were incubated with a polyclonal anti aldosterone synthase antibody (132) (kindly provided by Dr. Celso Gomez Sanchez) raised either in rabbit or sheep; or a polyclonal rabbit anti-Task3 antibody (Alomone Labs, Jerusalem, Israel) overnight at 4°C. Antibody incubation was performed in PBS supplemented with 0.04% of Triton-X100 and 0.5% bovine serum albumin (BSA). After removal of unbound primary antibody by washing with PBS, Cy2 donkey anti-rabbit or Cy2 donkey anti-sheep (Dianova, Hamburg, Germany) or Alexa Fluor 555 donkey anti-rabbit IgG (H+L) (Invitrogen, Germany) were used as secondary antibodies. The sections were then examined with a filter wheel-based imaging system (Universal Imaging Corporation, Dowingtown, PA, USA) mounted on an inverted microscope (Axiovert 200M; Carl Zeiss, Heidelberg, Germany) equipped with filters 31001 FITC and 31002 TRITC (Chroma Technology Corporation, Vermont, USA).

3.4 Adrenal gland perifusion

Adult Task3$^{+/+}$ and Task3$^{-/-}$ mice were anesthetized as previously described and both adrenal glands were removed. Adrenals were then cut into four pieces and incubated at

37°C in a Pasteur pipette containing Sephadex G50 (Sigma-Aldrich, Munich, Germany) embedded in control solution (each 100 ml of control solution contains: 46.9 ml of DMEM Low Glucose 31885 (Gibco, Darmstadt, Germany) and 53.1 ml of Krebs-HEPES solution (75 NaCl, 1.8 $CaCl_2$, 0.8 $MgSO_4$, 25 $NaHCO_3$, 1 Na_2HPO_4, 20 HEPES in mM) with a final K^+ concentration of 2.5 mM. D-Glucose; BSA and NaCl were added to obtain a final concentration of 1.5 mg/ml; 0.1 mg/ml and 135.5 mM respectively (0.85 ml of 1M NaCl solution for control buffer). For higher K^+ concentrations NaCl was replaced by KCl as necessary. The different solutions were pre-gazed with medical carbogen (5% CO_2 and 95% O_2) and applied at a constant flow rate of 0.15 ml/min and collected every 10 min for aldosterone measurements.

The perifusion setup can be schematized as follows:

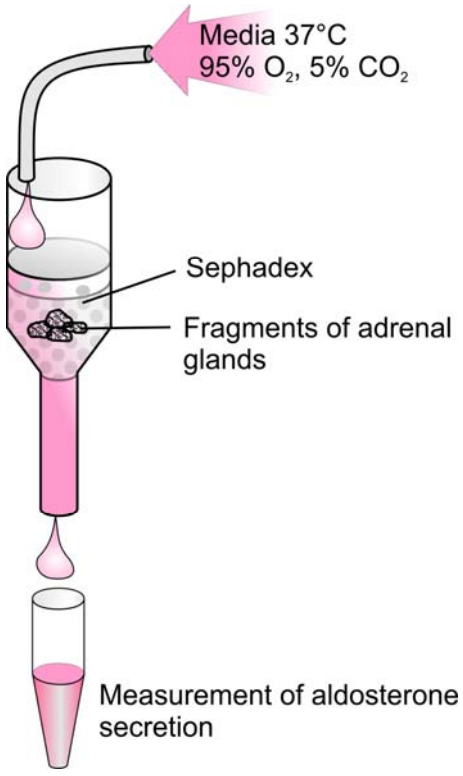

Figure 3.2. Schematic representation of the adrenal gland perifusion setup.

3.5 Primary cell culture

During isoflurane anesthesia, adult male Task3$^{+/+}$ and Task3$^{-/-}$ mice were perfused (see section 3.3 for details) with a collagenase-containing (0.5 mg/ml collagenase II (Biochrome, Berlin, Germany) and 0.5 mg/ml collagenase IV (Sigma-Aldrich, Munich, Germany)) Ringer-

type solution (see section 3.6 for details). Adrenal glands were harvested, cut into small pieces, and digested for another 10 min at 37°C. Single cells and cell clusters were seeded on culture dishes (Falcon, Heidelberg, Germany) in DMEM/F-12 (1:1) (Gibco, Darmstadt, Germany) supplemented with: 2% heat inactivated fetal calf serum (Gibco, Darmstadt, Germany), 8% heat inactivated horse serum (Gibco, Darmstadt, Germany), 0.1 mM ascorbic acid (Sigma-Aldrich, Munich, Germany), 1 µM (+)-α-Tocopherol (Sigma-Aldrich, Munich, Germany), 1 µg/ml human insulin solution (Sigma-Aldrich, Munich, Germany) and 0.5% Penicillin/Streptomycin (Gibco, Darmstadt, Germany). Cells were used for patch-clamp or calcium measurements experiments 16–24 h after seeding. Steroidogenic cells were identified by the presence of lipid droplets in the cytoplasm.

3.6 Electrophysiology

Whole-cell recordings were performed on primary cells using an EPC-10 amplifier (Heka, Lambrecht, Pfalz, Germany) coupled to a personal computer and a Powerlab Data Acquisition System (ADInstruments GmbH, Spechbach, Germany). The software PatchMaster v2x50 was used for pulse generation and data acquisition whereas the LabChartPro v7 was used for additional data acquisition. Patch pipettes (8-12) MΩ were used for the recordings. The patch pipette solution contained (in mM) 95 K-gluconate, 30 KCl, 4.8 Na_2HPO_4, 1.2 NaH_2PO_4, 5 glucose, 2.38 $MgCl_2$, 0.726 $CaCl_2$, 1 EGTA, 3 ATP, pH 7.2. The extracellular Ringer-type control solution contained (in mM) 142.5 NaCl, 0.4 NaH_2PO_4, 1.6 Na_2HPO_4, 5 glucose, 1 $MgCl_2$, 1.3 $CaCl_2$, 5 HEPES, 2.5 KCl, pH 7.4. All the experiments were performed at room temperature (RT).

The clamping protocol can be schematized as follows:

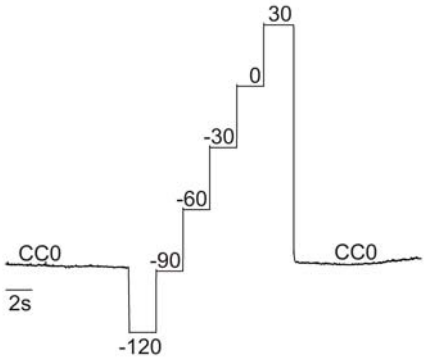

Figure 3.3. Schematic representation of the voltage clamp protocol applied. Voltage clamps ranging from -120 to 30 mV were applied every 2 seconds. Each clamp cycle was followed by 10 sec under current clamp 0 (CC0) condition to allow the measurement of the membrane voltage (whole cell mode).

3.7 Cytoplasmic Ca^{2+} measurements

3.7.1 Cytoplasmic Ca^{2+} measurements in fresh adrenal slices.

For cytoplasmic Ca^{2+} measurements in adrenal slices, adrenal glands from adult male mice were harvested during isoflurane anesthesia. Adrenals were then immediately placed in chilled storage solution containing (in mM) 26 $NaHCO_3$, 116.5 NaCl, 1.25 NaH_2PO_4, 10 Glucose, 2 $MgCl_2$, 1 $CaCl_2$, 2.5 KCl, pre-gazed with medical carbogen. After removal of surrounding fat tissue, the glands were embedded in 2% Biozym Plaque GP low melting agarose (Biozym, Hessisch Oldendorf, Germany) dissolved in storage solution at 37°C. After cooling down on ice, blocks of agarose containing the glands were cut into 150 µm thick slices using a vibratome VT 1200 S.(Leica, Wetzlar, Germany). Slices were kept for a maximum of 5 h in storage solution gazed with carbogen.

The slices were loaded with 2.5 µM Fluo-4 AM Ca^{2+} sensitive dye in the presence of 1X Power Load permeabilizing reagent (Invitrogen, Germany). The loading was performed in a Ringer type buffer containing (in mM) 5 HEPES, 138.9 NaCl, 1.6 Na_2HPO_4, 5.4 NaH_2PO_4, 10 Glucose, 1 $MgCl_2$, 1.3 $CaCl_2$, 3.6 KCl, pH 7.4. Loading periods of 40 min in an O_2 rich and humid atmosphere at room temperature were used. Slices were then rinsed for another 40 min in storage solution.

Emitted fluorescence was measured at 520 nm after 495 nm excitation (filter set 44 from Carl Zeiss, Jena, Germany), using a Lambda DG-4 illumination system (Sutter Instrument

Company, Ca. USA). An up-right microscope (Zeiss Examiner A1) equipped with a WN-Achroplan 40X water immersion objective (Carl Zeiss, Jena, Germany) was used for the measurements. The microscope was coupled to an Axiocam Mrm camera (Carl Zeiss, Jena, Germany). The images were continuously acquired each 0.5 seconds using the software Axiovision release 4.8.2 (Carl Zeiss, Jena, Germany). All measurements were performed at room temperature in the Ringer-type buffer gazed with O_2.

After acquisition of time laps experiments, the signal intensity emitted by single cells was measured using the Axiovision software. The initial intensity of the cells was drastically influenced by dye loading; therefore the signals measured during the experiment were normalized to the initial value. The Ca^{2+} sensitive dye Fluo-4 AM is prone to photobleaching and this phenomenon was observed during the experiments. Consequently, a baseline was subtracted from the fluorescence signal of the cells.

3.7.2 Cytoplasmic Ca^{2+} measurements in adrenocortical primary cells

For cytoplasmic Ca^{2+} measurements of adrenocortical primary cells, cells were loaded with 5 µM of Fura-2 AM in the presence of 1X Power Load permeabilizing reagent (Molecular Probes, Darmstadt, Germany). Cells were kept at room temperature in a Ringer-type solution previously described in section 3.7.1. Fluorescence was measured at 510 nm (filter set 21HE from Carl Zeiss, Jena, Germany) following excitation at 340 and 380nm. For this purpose, the setup described in the section 3.7.1 was used and images were continuously acquired (1 image/s). The ratio 340/380 was used as an indicator of the changes in $[Ca^{2+}]_i$.

3.8 Real-time polymerase chain reaction (real time-PCR)

Adrenal gland total RNA was isolated using RNeasy micro kit (Qiagen, Hilden, Germany) and reverse transcribed into cDNA using M-MLV reverse transcriptase (Promega, Mannheim, Germany). With Task3-specific primers (sense primer: ACATCAGCTCCGATGACTACC; antisense primer: CAGGTGCAGCATGTCCATA; annealing temperature 57°C, 50 cycles) real time-PCR was performed using SYBR green (Qiagen, Hilden, Germany). Beta-actin was used as a house-keeper gene (sense primer: CCA CCG ATC CAC ACA GAG TAC TT; antisense primer: GAC AGG ATG CAG AAG GAG ATT ACT G; annealing temperature 56°C, 40 cycles) in a LightCycler 480 machine (Roche, Basel, Switzerland).

3.9 Statistics

Data are shown in mean values ± standard error of the mean (SEM); “n” stands for the number of observations. Paired as well as unpaired Student’s t-tests were used accordingly. For multiple comparisons, one way ANOVA was used. A p-value of 0.05 was accepted to indicate statistical significance.

4. Results

4 Results

4.1 Expression and localization of Task3 in the mouse adrenal gland

The adrenal gland has been described as an organ with very strong expression levels of Task1 and Task3 channels (65). Interestingly, differences between genders have been found regarding the mRNA levels of Task3 in male and female mice (66). The following set of experiments aimed to investigate the expression of Task3 in the adrenal gland as well as its localization in the adrenal cortex.

4.1.1 Task3 mRNA expression in mouse tissues

Task3 mRNA expression in different mouse tissues was addressed by real time-PCR using specific primers (Figure 4.1).

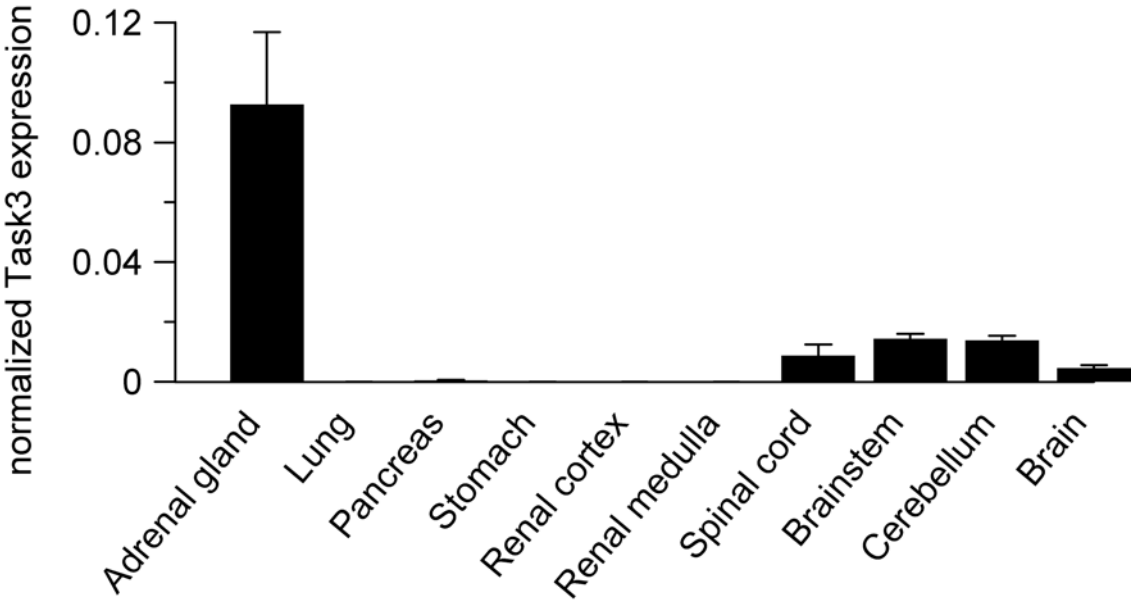

Figure 4.1. Expression of Task3 mRNA in different mouse tissues (n=3 mice) normalized to beta actin mRNA levels. Data obtained by InesTegtmeier and included with permission.

As shown in Figure 4.1, the adrenal gland is the primary site of Task3 expression in the mouse relatively to other tissues. Beside the adrenals, only tissues from the central nervous system express significant amounts of Task3 mRNA.

4.1.2 Task3 localization in the adrenal cortex

The specific localization of Task3 within the adrenals was investigated at the protein level through immunofluorescence (Figure 4.2).

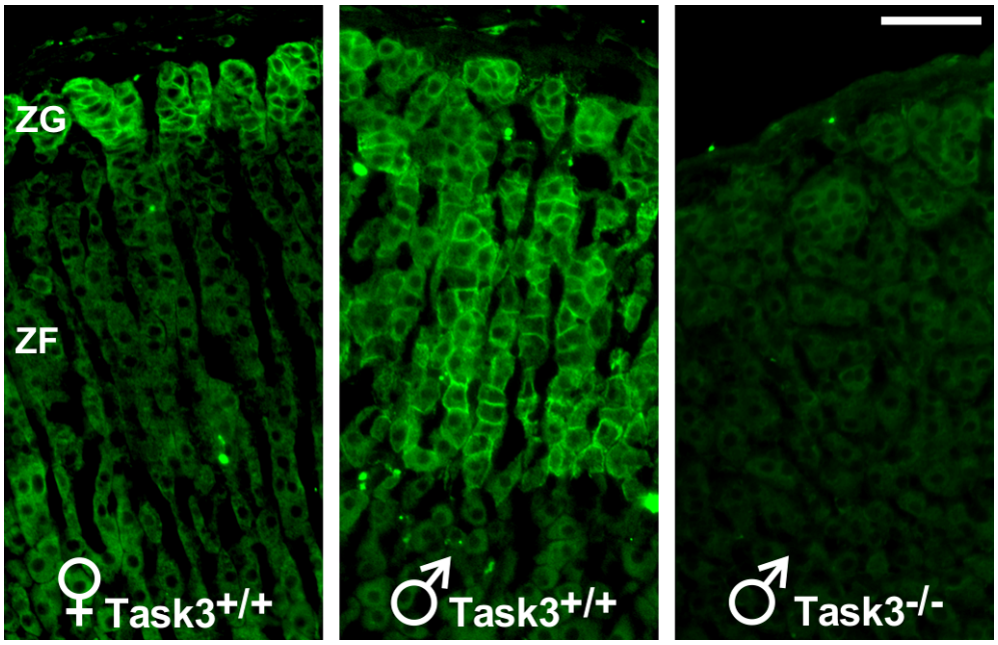

Figure 4.2. Localization of Task3 protein in the adrenal cortex. Task3 (green) localization was addressed in the adrenal glands of female (♀ $Task3^{+/+}$ n=5) and male (♂ $Task3^{+/+}$ n=5) wild type mice by immunofluorescence. Typical sections are depicted. The specificity of the used antibody was tested by staining the adrenal glands of male Task3 knockout mice (♂ $Task3^{-/-}$ n=3). In the figure, ZG: *zona glomerulosa*; ZF: *zona fasciculata*. The bar corresponds to 50 µm.

Task3 staining was found in the adrenal cortex of both genders. Task3 positive cells in the adrenal cortex exhibited strong membrane staining. *Zona glomerulosa* cells, organized in their typical "rosetta" structure beneath the capsule, were stained regardless of the gender. In male mice, Task3 expression was also found in *zona fasciculata* cells typically arranged in radial columns (middle panel). The specificity of the antibody was confirmed in samples from $Task3^{-/-}$ male mice (right panel).

4.1.3 Dynamics of Task3 expression in the adrenal cortex

To test whether the sex dependent localization of Task3 was caused by male sex hormones, wild type male mice were castrated and adrenal slices prepared for immunofluorescence. Task3 localization was compared between animals treated with

the vehicle (n=6) and those treated with testosterone propionate (n=6) (Figure 4.3 A). Sham operated animals (n=3) were used as control.

Conversely, female mice were treated with vehicle (n=3) or testosterone propionate (n=3) and the expression of Task3 was then investigated by immunofluorescence (Figure 4.3B).

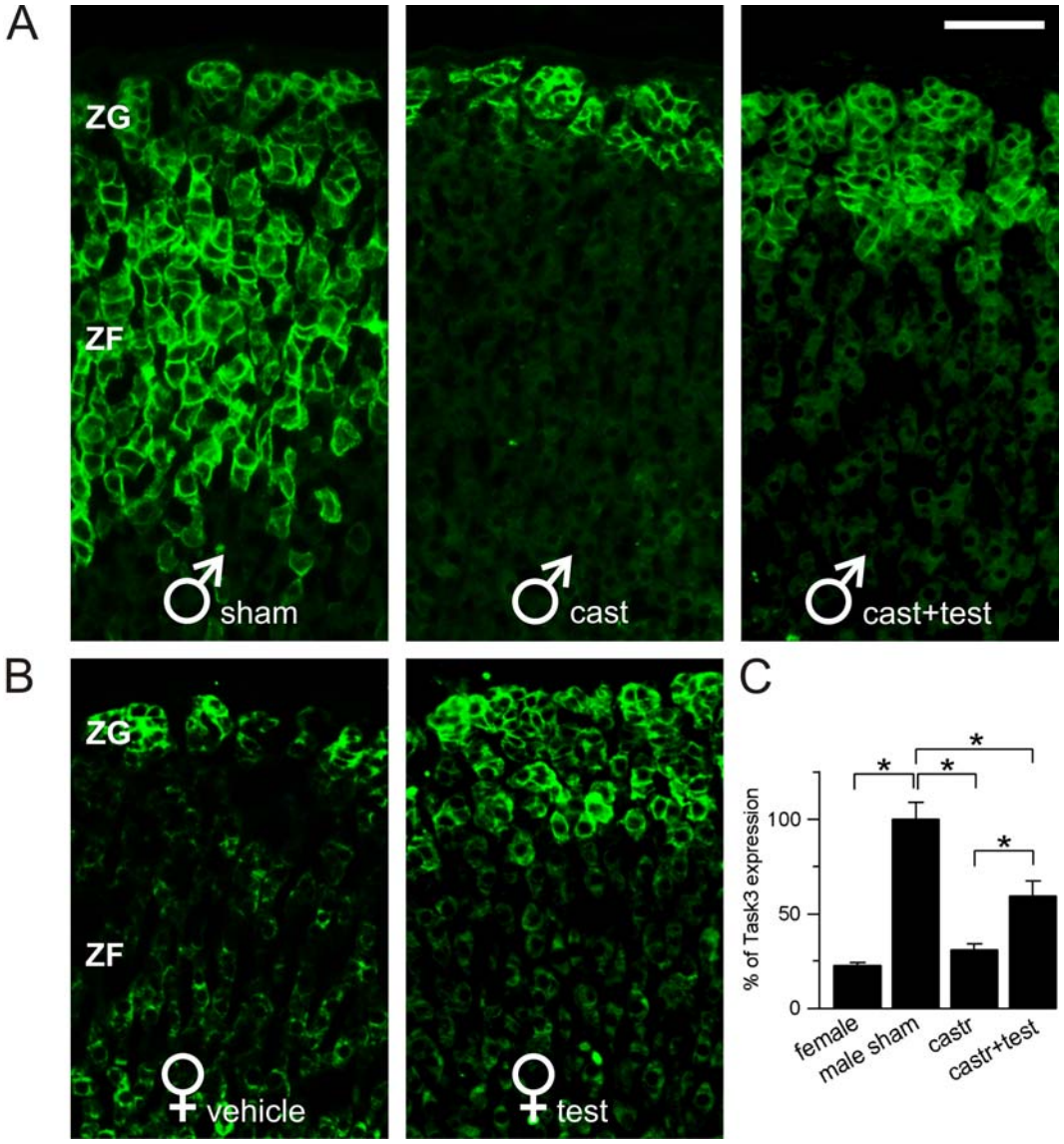

Figure 4.3. Effects of castration and testosterone treatment on the adrenal expression and localization of Task3. Typical sections are shown. **A**: Task3 Immunofluorescence (green) was assessed in male mice. Animals were sham operated and treated with vehicle (♂ sham) or castrated and treated with vehicle (♂ cast) or with testosterone propionate (♂ cast+test). **B**: Task3 Immunofluorescence (green) in adrenal glands of female mice treated with testosterone

propionate (♀ test) or vehicle (♀ vehicle). In both **A** and **B** panels ZG: *zona glomerulosa;* ZF: *zona fasciculata* and the scale bar correspond to 50 µm. **C**: Expression of Task3 mRNA in the adrenals of wild type female mice (female) (n=7); male mice sham operated and treated with vehicle (male sham) (n=8); male animals castrated and treated with vehicle (castr) (n=6); male animals castrated and treated with testosterone propionate (castr+test) (n=6). Values are expressed in percentage. The 100% corresponds to the expression of Task3 in the sham operated males. Asterisks indicate statistically significant differences ($p \leq 0.05$). The real time-PCR data was contributed by Dr. Sascha Bandulik and included with permission.

Remarkably, the expression of Task3 was drastically changed in male mice after castration. In these animals, the expression of Task3 was abolished in *zona fasciculata* and only remained in *zona glomerulosa* cells (Figure 4.3. A middle panel). On the other hand, in sham operated male mice, the localization of Task3 was as in non-treated male animals, exhibiting a strong membrane staining in both *zona glomerulosa* and *zona fasciculata* cells (Figure 4.3. A left panel). Impressively, treatment of castrated mice with testosterone propionate partially recovers the expression of Task3 in deeper cells belonging to *zona fasciculata* (Figure 4.3. A right panel). A similar effect of testosterone was observed in female mice, where the normal localization of Task3 is mainly in *zona glomerulosa* cells (Figure 4.3. B left panel). Following treatment with testosterone propionate, a deeper expression within the *zona fasciculata* was detected in females (Figure 4.3. B right panel). These results were corroborated by the analysis of Task3 mRNA expression using real time-PCR (Figure 4.3. C).

4.2 Expression and localization of aldosterone synthase in the adrenal cortex

Task1 invalidation causes an inappropriate localization of the aldosterone synthase in the adrenal gland of adult female mice (66). Therefore, we addressed the question whether a similar defect occurs as a consequence of Task3 deletion. The localization of the aldosterone synthase in the adrenal cortex was investigated through immunofluorescence (Figure 4.4).

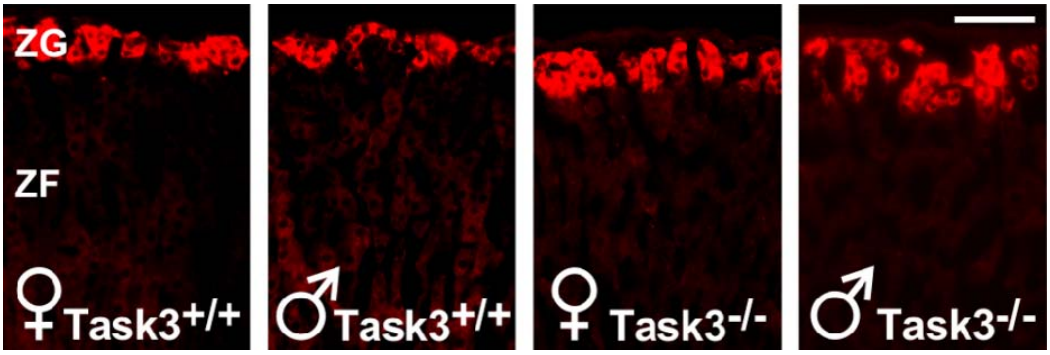

Figure 4.4. Localization of aldosterone synthase (red) in the adrenal cortex from wild type (Task3$^{+/+}$) and Task3 knockout (Task3$^{-/-}$) mice. A specific polyclonal antibody raised in sheep was used for aldosterone synthase staining in Task3$^{+/+}$ mice. A similar antibody raised in rabbit against the same epitope was used in Task3$^{-/-}$ mice. In the figure, ZG: *zona glomerulosa;* ZF: *zona fasciculata*. Scale bar corresponds to 50 µm.

As shown in the figure 4.4, aldosterone expression and localization was conserved after Task3 deletion.

4.3 Contribution of Task3 K^+ channels to the K^+ sensitivity of adrenocortical cells and tissues

Task channels set the background K^+ conductance and are therefore crucial for the maintenance of membrane voltage in glomerulosa cells. The following set of experiments was aimed at investigating the impact of Task3 deletion on the K^+ sensitivity of adrenocortical primary cells and freshly isolated adrenocortical tissue. To this end, *in vitro*, as well as *ex vivo* approaches were used.

4.3.1 Effect of $[K^+]_o$ on the membrane voltage and intracellular Ca^{2+} signaling of adrenocortical primary cells

The patch clamp technique was used to investigate the effects of Task3 deletion on the membrane potential of adrenocortical primary cells (Figure 4.5). Different $[K^+]_o$ were used to explore the potassium sensitivity of these cells.

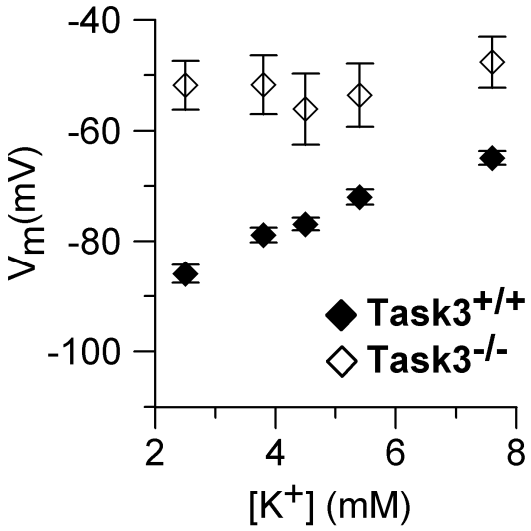

Figure 4.5. Effect of $[K^+]_o$ on the membrane voltage (V_m) of adrenocortical cells from Task3$^{-/-}$ (n=5-9) and Task3$^{+/+}$ (n=9-13) male mice.

Task3$^{+/+}$ cells were hyperpolarized at a $[K^+]_o$ of 2.5 mM (-87.0 ± 1.42 mV; n=16) compared to Task3$^{-/-}$ cells (-47.82 ± 2.77 mV; n=19). In Task3$^{+/+}$ cells, the V_m followed the changes in $[K^+]_o$, acting like a $[K^+]_o$ sensitive electrode. On the other hand, in Task3$^{-/-}$ cells the V_m was barely affected after changes of the $[K^+]_o$.

Additionally, another approach was used to assess, the K^+ sensitivity of adrenocortical primary cells by investigating the $[Ca^{2+}]_i$ response following increase in $[K^+]_o$ using Fura-2 fluorescence (Figure 4.6).

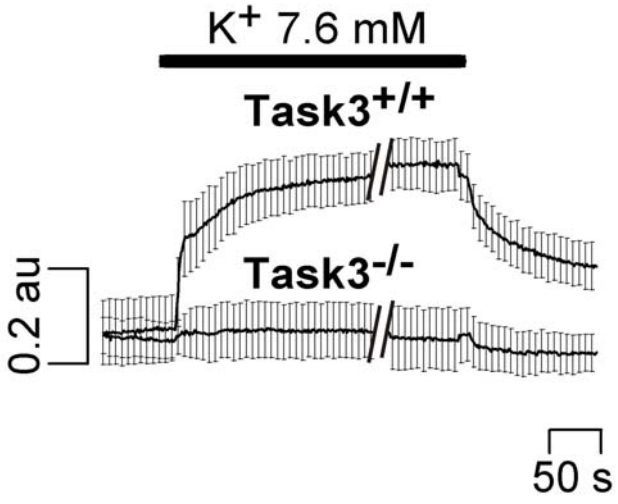

Figure 4.6. Effect of 7.6 mM $[K^+]_o$ on the $[Ca^{2+}]_i$ of adrenocortical cells from Task3$^{-/-}$ (n=7) and Task3$^{+/+}$ (n=6) male mice. Mean values ± SEM of the Fura-2 ratio 340/380 are represented in arbitrary units (au).

As expected, after subjecting Task3$^{+/+}$ cells to supraphysiological $[K^+]_o$, the $[Ca^{2+}]_i$ increased in a sustained way due to Ca^{2+} influx. In contrast, in Task3$^{-/-}$ cells only a slight increase in $[Ca^{2+}]_i$ was observed. It is worth noting that cells from both genotypes have a similar $[Ca^{2+}]_i$ under non stimulated conditions.

4.3.2 Effect of $[K^+]_o$ on the cytoplasmic Ca^{2+} signaling of glomerulosa cells in fresh adrenal slices

The identification of glomerulosa cells in a mixed primary adrenocortical culture is a complex issue, since they represent a minority of the steroid producing cells in the adrenal cortex. Moreover, it is well known that cells in primary culture are prone to de-differentiation, which include changes in their morphological and functional characteristics. To overcome this, we developed an acute adrenal preparation which allowed us the unequivocally identification of *zona glomerulosa* cells, and the measurement of $[Ca^{2+}]_i$ in a more physiological scenario. Fresh adrenal slices from Task3$^{+/+}$ (n=3 slices/2 mice) and Task3$^{-/-}$ (n=9 slices/2 mice) mice were loaded with the Ca^{2+} sensitive dye Fluo-4 AM. The changes in the $[Ca^{2+}]_i$ were measured upon stimulation with $[K^+]_o$ of 7.6 mM (Figure 4.7), being 2.5 mM the $[K^+]_o$ under control conditions.

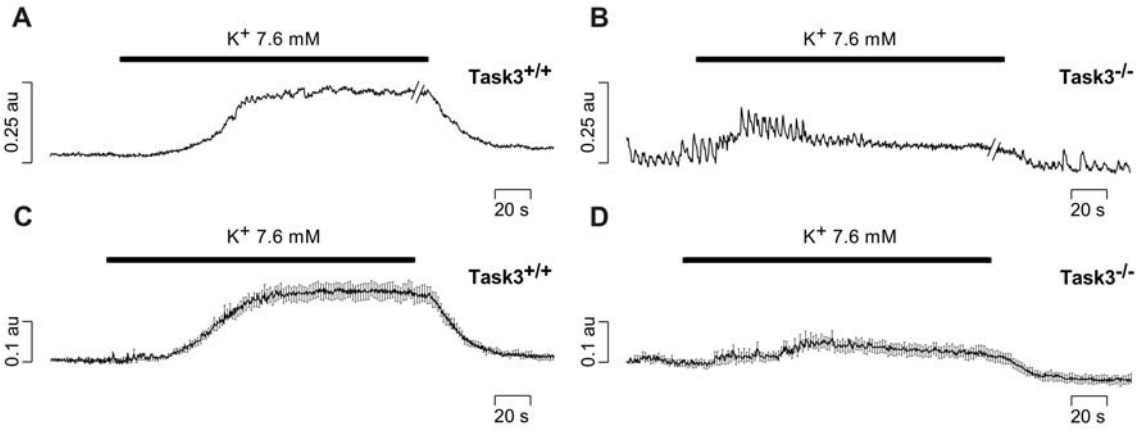

Figure 4.7. Measurement of $[Ca^{2+}]_i$ in acute adrenal slices from Task3$^{+/+}$ and Task3$^{-/-}$ mice after stimulation with $[K^+]_o$=7.6 mM. Typical traces corresponding to Task3$^{+/+}$ (**A**) and Task3$^{-/-}$ (**B**) cells are shown. Traces representing mean values ± SEM of at least 3 independent experiments of Task3$^{+/+}$ and Task3$^{-/-}$ adrenal slices are shown in **C** and **D** respectively. au: arbitrary units.

The increase observed in the $[Ca^{2+}]_i$ was larger in $Task3^{+/+}$ than in $Task3^{-/-}$ cells, confirming the observations already made in adrenocortical primary cells.

One of the most striking findings was that glomerulosa cells from $Task3^{-/-}$ slices showed an increased spontaneous Ca^{2+} activity compared to $Task3^{+/+}$ cells. As it is evident in Figure 4.7. B, even without any stimulation, some of the $Task3^{-/-}$ cells exhibit bursting Ca^{2+} activity which was less frequently observed in $Task3^{+/+}$ cells (this was also evident in another series of experiments shown in Figure 4.10). This activity results in an increased scattering of the baseline obtained in $Task3^{-/-}$ slices (Figure 4.7 D) when compared to $Task3^{+/+}$ ones (Figure 4.7A).

4.3.3 Effect of $[K^+]_o$ on the aldosterone secretion of perifused adrenal tissue

Membrane depolarization followed by an increase of the $[Ca^{2+}]_i$ are primary events in glomerulosa cells when stimulated by hyperkalemia. We then investigated the impact of the deletion of Task3 potassium channels for the aldosterone secretion by the adrenal glands. To this end, we developed a device which allowed an *ex vivo* stimulation of adrenal tissue with different $[K^+]_o$ followed by sequential measurement of the aldosterone secretion. Through this approach, the stimulation takes place in a scenario closely resembling the *in vivo* conditions. At the same time potential compensatory mechanisms present in the whole animal are circumvented.

After equilibrating the tissue for 1,5 h with a solution containing 2.3 mM of K^+, stepwise increases in $[K^+]_o$ were applied to stimulate the aldosterone production in freshly harvested adrenals from male and female $Task3^{+/+}$ and $Task3^{-/-}$ mice (Figure 4.8).

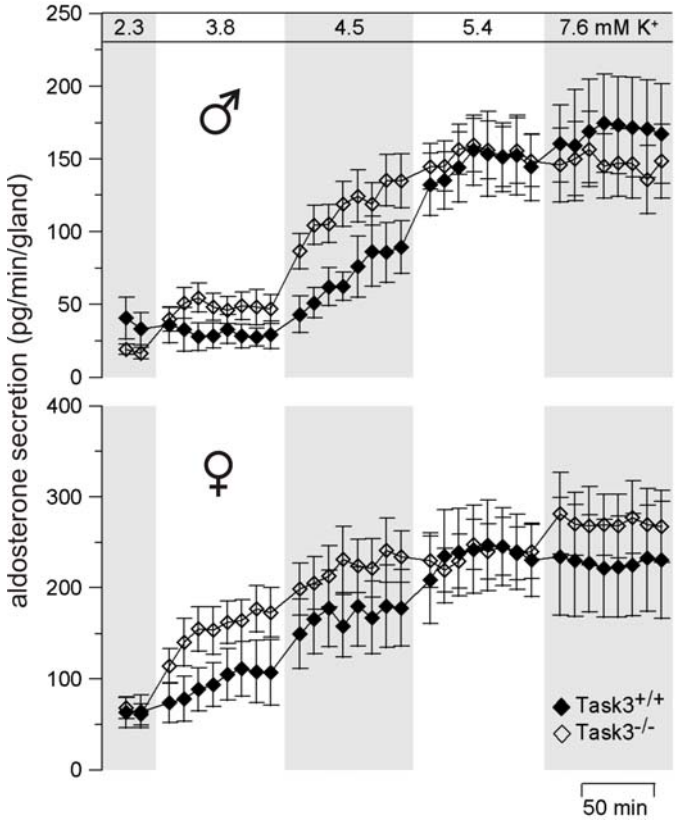

Figure 4.8. Aldosterone secretion by *ex vivo* perifused adrenal glands from Task3$^{+/+}$ (n=5 ♂ and 6 ♀) and Task3$^{-/-}$ (n=5 ♂ and 8 ♀) mice. Mean values ± SEM of the aldosterone secreted by one adrenal in one minute are shown.

Notably, adrenal glands from females secrete more aldosterone than those from male animals, probably due to their larger size (133). Regardless of the gender, there were no major differences between Task3$^{+/+}$ and Task3$^{-/-}$ glands concerning the aldosterone secretion in response to increase of $[K^+]_o$. The most remarkable difference between genotypes was that Task3$^{-/-}$ adrenals were more sensitive to stimulation with 3.8 mM of $[K^+]_o$ than Task3$^{+/+}$ ones, which could indicate a modified "tuning" of the secretory response.

4.4 Contribution of Task3 K^+ channels to the response of adrenocortical cells and tissue upon AngII stimulation

AngII promotes Ca^{2+} influx in glomerulosa cells via the inhibition of K^+ conductance and consequent cell depolarization, leading to opening of voltage gated Ca^{2+} channels. Additionally, AngII induces a release of Ca^{2+} from intracellular stores. The following

experimental sets aimed at investigating the contribution of Task3 K^+ channels to the AngII inhibitable K^+ conductance. The intracellular Ca^{2+} signaling in adrenocortical primary cells and tissues was also studied.

4.4.1 Impact of Task3 deletion on electrophysiological parameters of adrenocortical primary cells

The patch clamp technique was used to investigate the effect of AngII in the V_m and whole cell currents of Task3$^{+/+}$ and Task3$^{-/-}$ adrenocortical primary cells (Figure 4.9).

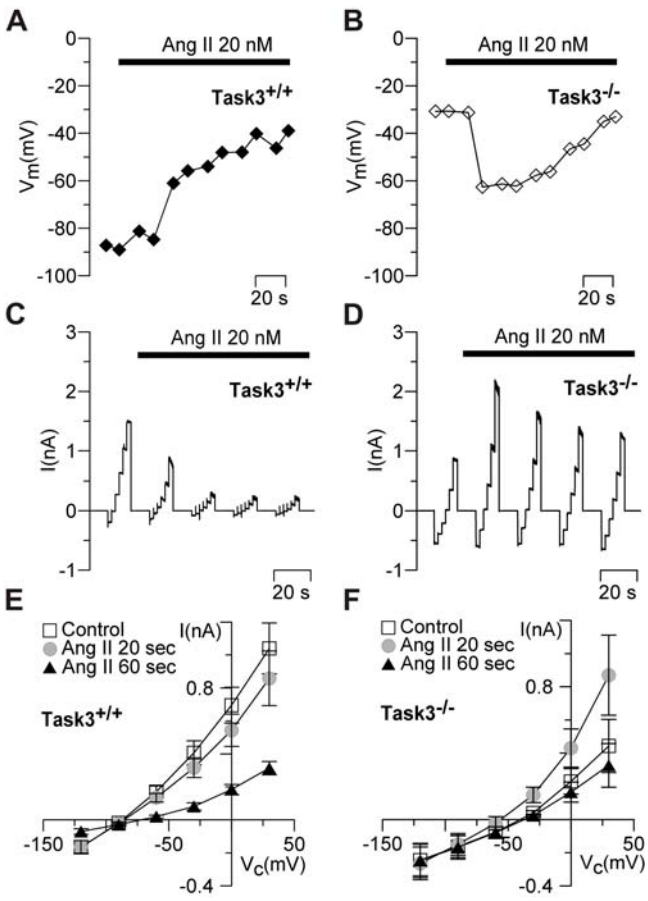

Figure 4.9. Effect of AngII on V_m and whole cell current (I) of Task3$^{+/+}$ and Task3$^{-/-}$ adrenocortical primary cells. Original traces of the effects produced by AngII on V_m in Task3$^{+/+}$ and Task3$^{-/-}$ adrenocortical primary cells are shown in **A** and **B**, respectively. Original traces of the effects of AngII on whole cell currents in Task3$^{+/+}$ and Task3$^{-/-}$ adrenocortical primary cells are shown in **C** and **D**, respectively. I/V relation of Task3$^{+/+}$ (n=8) (**E**) and Task3$^{-/-}$ (n=9) (**F**) adrenocortical primary cells upon AngII stimulation. Mean values ± SEM of the whole cell conductance are shown before the application of AngII (control, open squares); 20 seconds after the application of AngII (Ang II 20 sec, gray circles) and 60 seconds after the application of AngII (Ang II 60 sec, black triangles).

As shown in Figure 4.9. A, addition of 20 nM of AngII to Task3$^{+/+}$ adrenocortical primary cells led to a strong depolarization, accompanied by a drastic reduction of whole cell current (Figure 4.9. C). The V_m shifted from -85.75 ± 1.68 mV to -62.75 ± 5.07 mV after 60 seconds (Figure 4.9. E).

Surprisingly, Task3$^{-/-}$ cells exhibited a transient hyperpolarization as a consequence of the application of AngII (Figure 4.9. B) instead of the depolarization observed in Task3$^{+/+}$ cells. These cells were depolarized under control conditions, as previously mentioned in section 4.3.1. AngII also increased the outward K^+ current in a transient manner (Figure 4.9. D). The V_m shifted from -44.72 ± 4.32 mV to -69.61 ± 6.37 mV, 20 seconds after the application of AngII (Figure 4.9. F). 40 seconds later the V_m was -33.25 ± 2.63 mV, slightly depolarized with respect to resting conditions.

Another interesting finding was that it was still possible to depolarize Task3$^{-/-}$ adrenocortical cells by extracellular acidification. After subjected to pH 6, Task3$^{-/-}$ adrenocortical cells depolarized from -49.7 ± 6.2 mV to -28.5 ± 4.3 mV. On the other hand Task3$^{+/+}$ cells depolarized from -84.5 ± 1.9 mV to -60.1 ± 6.7 mV when subjected to acidic pH.

4.4.2 Effect of AngII on the cytoplasmic Ca^{2+} signaling of glomerulosa cells in acute adrenal slices

Whether Task3 deletion modifies the Ca^{2+} signaling triggered by AngII in glomerulosa cells was also investigated. To this end Task3$^{+/+}$ (n=6) and Task3$^{-/-}$ (n=6) acute adrenal slices were used. The changes in $[Ca^{2+}]_i$ were analyzed by loading the cells with the Ca^{2+} sensitive dye Fluo-4 AM (Figure 4.10).

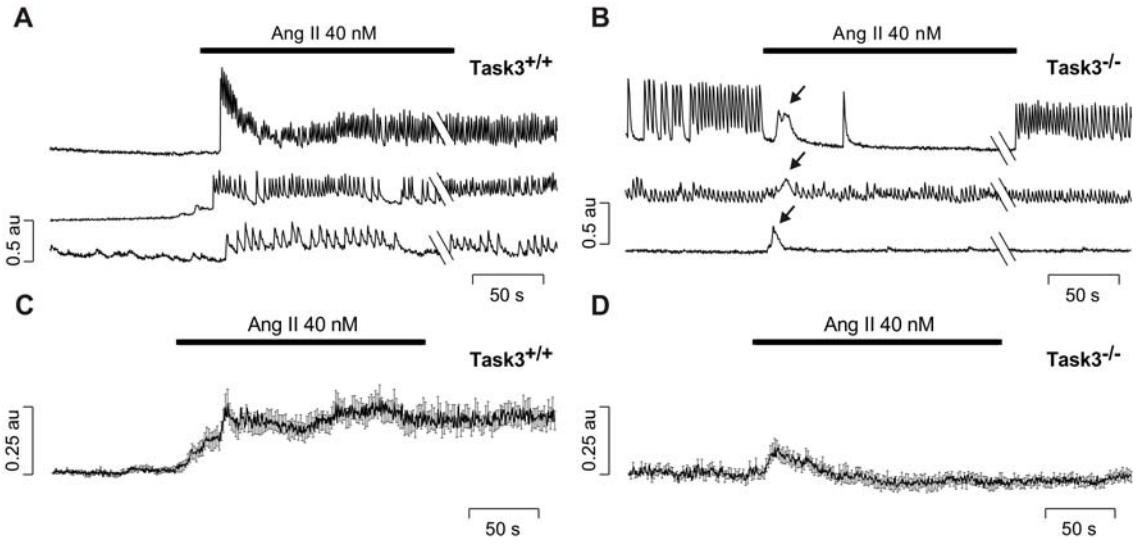

Figure 4.10. $[Ca^{2+}]_i$ changes elicited in *zona glomerulosa* cells upon AngII stimulation. Original traces of three typical Task3$^{+/+}$ (**A**) and Task3$^{-/-}$ (**B**) glomerulosa cells. **C** and **D**: Mean values ±

SEM of $[Ca^{2+}]_i$ of six Task3$^{+/+}$ and Task3$^{-/-}$ experiments. Values are expressed in arbitrary units (au).

AngII promoted an increase of $[Ca^{2+}]_i$ in Task3$^{+/+}$ glomerulosa cells (Figure 4.10. A and C). Although the intracellular Ca^{2+} signaling was found to be variable among different Task3$^{+/+}$ cells (see the three examples in figure 4.10 A); these cells were generally silent before stimulation. A bursting activity was elicited upon addition of AngII. Remarkably, this stimulation was poorly reversible during the 3 min washing period after AngII.

On the other hand Task3$^{-/-}$ glomerulosa cells exhibited a severely disturbed intracellular Ca^{2+} signaling (Figure 4.10. B). In contrast to Task3$^{+/+}$ traces, cytoplasmic Ca^{2+} of Task3$^{-/-}$ under baseline conditions was often rather unstable due to spontaneous oscillations of $[Ca^{2+}]_i$, as already described in section 4.3.2. The intracellular Ca^{2+} signaling also varied among different Task3$^{-/-}$ cells. The upper trace of the Figure 4.10. B is characteristic of a group of cells exhibiting a strong spontaneous Ca^{2+} activity, which is silenced upon the addition of AngII. A broader peak (indicated with an arrow) appears immediately after stimulation, which might correspond to store release of Ca^{2+} from the ER. The trace in the middle is typical from a group of cells with spontaneous activity which was not silenced by AngII. Finally, the last trace is characteristic from cells exhibiting a stable baseline and a transient peak (indicated with an arrow) after AngII stimulation.

In Figure 4.10. D, the summary of the intracellular Ca^{2+} activity in Task3$^{-/-}$ glomerulosa cells is shown. Notably the scattering of the Ca^{2+} activity under baseline conditions was larger in these cells compared to Task3$^{+/+}$ cells (Figure 4.10. B). Remarkably, only a transient $[Ca^{2+}]_i$ increase was elicited in Task3$^{-/-}$ cells by AngII, the plateau phase was virtually absent.

4.5 Phenotype of Task3$^{-/-}$ mice

As showed in the previous sections of this chapter, the deletion of Task3 K^+ channels impaired cellular processes involved in the regulation of aldosterone secretion. In the experimental sets of the following sections, the main goal was to investigate the systemic impact of Task3 deletion on the aldosterone regulation in living mice.

4.5.1 Effect of dietary K^+ on plasma aldosterone concentrations

K^+ rich and K^+ depleted diets were used to investigate the impact of Task3 deletion on the K^+ sensitivity of aldosterone secretion in living mice (Figure 4.11).

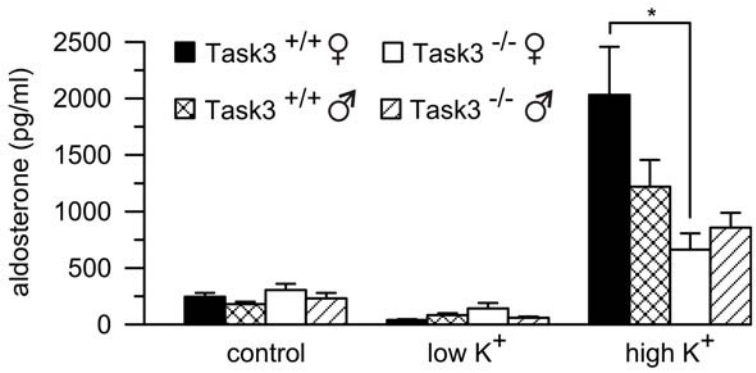

Figure 4.11. Plasma aldosterone concentrations of Task3$^{+/+}$ (n=14-26) and Task3$^{-/-}$ (n=11-21) mice subjected to normal (control), low K^+ or high K^+ diets. The asterisk indicates a statistically significant difference ($p \leq 0.05$). Data contributed by Prof. Dr. Jacques Barhanin and Dr. Sascha Bandulik, included with permission.

Under control conditions, Task3$^{+/+}$ and Task3$^{-/-}$ animals had similar concentrations of aldosterone in plasma. After reduction of K^+ in the diet, animals from both genotypes were able to reduce the secretion of aldosterone to a similar extent.

On the other hand, Task3$^{+/+}$ animals secreted more aldosterone when subjected to K^+ rich diets, comparatively to control diet. Although Task3$^{-/-}$ mice were also able to increase the plasma aldosterone concentrations upon a K^+ rich diet, they were not able to do it to the same extent as Task3$^{+/+}$ animals. Interestingly, this difference was more pronounced in females, although in males the tendency was also present.

4.5.2 Effect of dietary Na^+ on plasma renin and aldosterone levels

Task3$^{+/+}$ and Task3$^{-/-}$ mice were subjected to diets with different concentrations of Na^+. Under these conditions plasma renin activity (PRA) and plasma aldosterone concentrations were measured and the aldosterone/renin ratio was calculated (Figure 4.12).

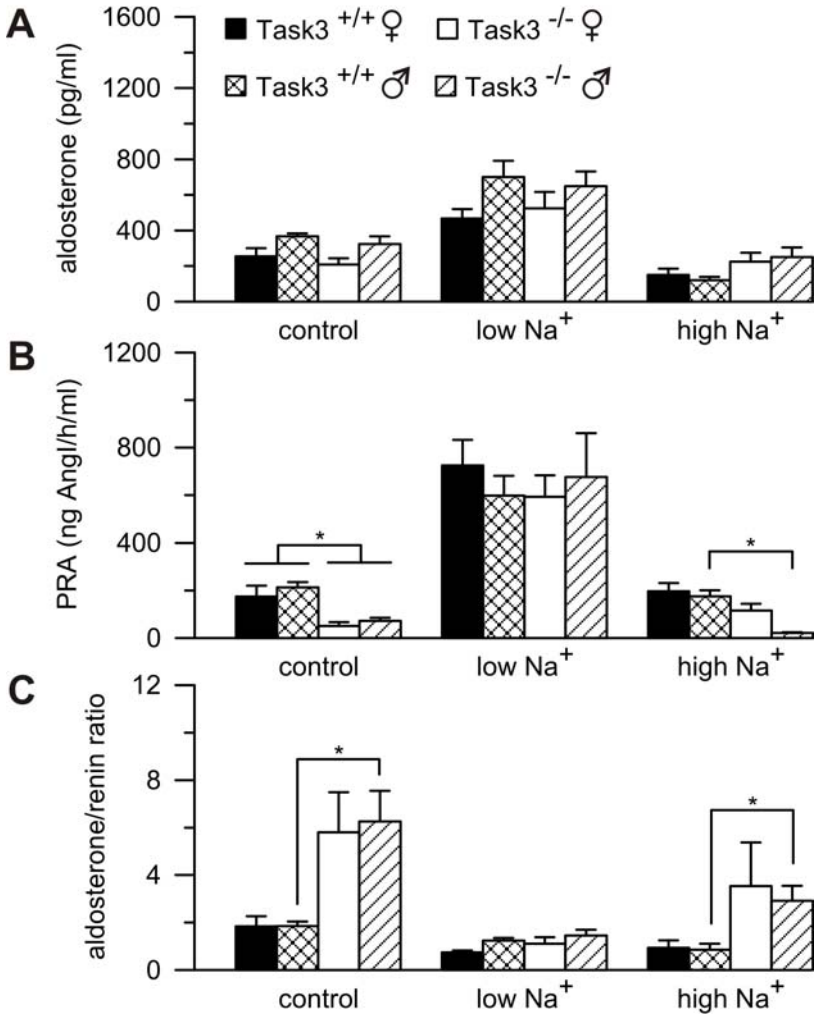

Figure 4.12. A: Plasma aldosterone concentrations of Task3$^{+/+}$ (n=6-13) and Task3$^{-/-}$ (n=5-10) mice under normal (control), deprived (low Na^+) and rich (high Na^+) Na^+ diets. **B** and **C**: Plasma renin activity and aldosterone/renin ratio of the same animals. Asterisks indicate statistically significant differences ($p \leq 0.05$). Data contributed by Prof. Dr. Jacques Barhanin; Prof. Dr. Frank Schweda and Dr. Sascha Bandulik, included with permission.

As summarized in Figure 4.12. A, Task3$^{+/+}$ as well as Task3$^{-/-}$ mice were able to increase their secretion of aldosterone to a similar extent in response to Na^+ deprivation. Similarly, the plasma concentrations of aldosterone in animals subjected to Na^+ rich diet were decreased to a similar extent in both genotypes. However it is noticeable, although not statistically significant, that Task3$^{-/-}$ mice secreted relatively higher amounts of aldosterone under high Na^+ diet.

These changes in aldosterone secretion reflected the changes in PRA in Task3$^{+/+}$ mice (Figure 4.12. B). Thus, PRA was increased in Task3$^{+/+}$ animals deprived of dietary Na^+

but it was similar to the control values of animals kept under high Na^+ diet. Surprisingly, $Task3^{-/-}$ animals exhibit a very low PRA under control conditions when compared to $Task3^{+/+}$. In $Task3^{-/-}$ mice subjected to Na^+ deprivation, the PRA increased to a similar extent as in $Task3^{+/+}$ mice. $Task3^{-/-}$ animals fed with a Na^+ rich diet exhibited lower PRA than $Task3^{+/+}$.

The ratio between the plasma aldosterone concentration and the PRA is a valuable tool for the diagnosis of primary hyperaldosteronism. It indicates whether aldosterone secretion is or not mainly regulated by the renin-angiotensin system. Thus, an elevated aldosterone/renin ratio suggests a (partially) autonomic secretion of aldosterone by the adrenal gland. This was the case of $Task3^{-/-}$ mice when subjected to control conditions or under a Na^+ rich diet. Under both diets they exhibited an increased aldosterone/renin ratio when compared to $Task3^{+/+}$. Male animals showed more pronounced differences, although in females the tendency is also apparent.

5. Discussion

5 Discussion

In the early fifties of the past century, Sylvia and her husband James Tait isolated and identified the molecule of “electrocortin” (later named aldosterone) from 500 Kg of beef adrenals (134; 135). After this seminal work, the Tait couple also pioneered the research of the metabolic pathways and the physiological effects of this and other steroids (135). Another milestone in the studies of aldosterone and its related pathophysiology was contributed by Jerome W. Conn who produced the first report of primary hyperaldosteronism (PA) in 1954 (136). Since then, numerous studies have addressed questions regarding aldosterone secretion, its physiological role and related pathologies.

Aldosterone is produced by *zona glomerulosa* cells from the adrenal cortex, which exhibit a very high K^+ conductivity and are thus strongly hyperpolarized under resting conditions. The two strongest secretagogues of aldosterone, hyperkalemia and angiotensin II, exert their actions (at least in part) by depolarizing aldosterone producing cells. The discovery of the K_2P family of potassium channels immediately raised the hypothesis that some of its members could participate in the K^+ sensitivity of glomerulosa cells. The K_2P channels Trek1, Task1 and Task3 have been found to be highly expressed in the adrenal cortex of several species. In the present work, the particular contribution of Task3 to the regulation of aldosterone secretion was investigated by using the Task3 knockout mouse model.

5.1 Task3 expression and localization in the adrenal cortex is sex dependent

In the present work we provide evidence supporting the conclusion that the adrenal gland is the organ exhibiting the highest level of Task3 expression in mice (see Figure 4.1). Moreover, Task3 was found to be expressed in the *zona glomerulosa* of the adrenal cortex. This finding supports the hypothesis that Task3 plays a role in the regulation of aldosterone production.

Interestingly, the expression and localization of Task3 in the adrenal cortex was found to be sex dependent. Remarkably, sex-related differences were also found previously in Task1$^{-/-}$ mice. Heitzmann and co-workers (66) found that only Task1$^{-/-}$ female mice

are affected with hypertension and hyperaldosteronism. These mice exhibited an ectopic localization of the aldosterone synthase enzyme in the *zona fasciculata* instead of the normal localization in the *zona glomerulosa*. In the same work, the authors proposed the possible role of Task3 as compensatory factor in male animals. In line with this hypothesis, we found that in females, Task3 is only expressed in *zona glomerulosa* cells, while in males it is also expressed in the cells of *zona fasciculata* (see Figure 4.2).

Heitzmann and co-workers also found that it was possible to rescue the normal zonation in female Task1$^{-/-}$ mice by treating them with testosterone. In line with these data, we found that testosterone promotes the expression of Task3 in *zona fasciculata* cells both in females and castrated male mice (see Figure 4.3).

At this point one might think that the explanation of the different phenotype exhibited by male and female Task1$^{-/-}$ mice could be described as follows: Task1, which is expressed throughout the whole adrenal cortex (65; 85) is a key factor controlling the normal localization of the aldosterone synthase. When Task1 is deleted, its close relative Task3 can take over its function. Since Task3 is expressed in *zona fasciculata* only in males, Task1$^{-/-}$ female animals are the most affected ones. The proof of concept to corroborate this hypothesis would have been a dezonated phenotype in Task1$^{-/-}$/Task3$^{-/-}$ male mice. However, some findings added a bit of complexity to this allegedly simple scenario.

Davies and co-workers (65) described the phenotype of Task1$^{-/-}$/Task3$^{-/-}$ mice and reported that males were normally zonated. By using immunofluorescence and *in situ* hybridization we confirmed that Task1$^{-/-}$/Task3$^{-/-}$ male mice express the aldosterone synthase only in *zona glomerulosa* (data not shown). Interestingly, these mice exhibit an apparent broadening of this zone; a feature which probably contributes to their hyperaldosteronism. On the other hand, the ectopic localization of the aldosterone synthase found in Task1$^{-/-}$ females was less prominent when Task3 was also deleted (data not shown).

It has been shown that testosterone has a crucial role in the plasticity and metabolism of the adrenal cortex. For instance, the activity of the 3β-hydroxysteroid dehydrogenase (the enzyme catalyzing the conversion of pregnenolone into progesterone), was found to be suppressed *in vivo* (137) and *in vitro* (138) by testosterone. Moreover, the *zona*

X, which is supposedly a reminiscence of the fetal adrenal zone (139), is also significantly influenced by testosterone. It degenerates in male mice after puberty, whereas in females it persists until the first pregnancy (133). This degeneration can be prevented by castration in male mice and can be promoted by androgen treatment in females (9). Nevertheless, the factors promoting the degeneration of *zona X* in females after the first pregnancy are not yet well understood.

Altogether these evidences strongly support the idea that the remodeling of the cellular and metabolic characteristics of the adrenal cortex is a fully dynamic process. Perhaps the effects of androgens have been the most studied but other overlooked factors such as age, nutritional state, stress etc. can also take part in this process. It is tempting to hypothesize that Task3 is probably involved in the compensatory effect observed in Task1$^{-/-}$ male mice, but certainly it is not the only element.

Another conflictive issue concerns the localization of Task3 in the male adrenal cortex. By using *in situ* hybridization Davies and co-workers (65) found Task3 mRNA exclusively in the *zona glomerulosa* cells. This finding was confirmed in our lab using a different probe (data not shown). However, here we report that at the protein level Task3 is also expressed in the *zona fasciculata*.

Remarkably, as shown in Figure 4.3, higher levels of protein detected by immunofluorescence corresponds to higher levels of mRNA measured by quantitative RT-PCR and vice versa. Furthermore, Heitzmann and co-workers also described gender dependent expression of Task3 using different primers for real time-PCR (66). In addition, Task3 mRNA levels were comparable in male and female before puberty (66) and at protein level; exclusive glomerulosa localization was found (data not shown).

It is striking that Task3 mRNA level is approximately four times higher in males than in females, as measured by RT-PCR by us and others (66). Since the *zona fasciculata* is far larger than the *zona glomerulosa*, a relatively low expression of Task3 mRNA levels in male fasciculata cells can account for the observed differences. It is thus possible that such levels are below the sensitivity threshold of an *in situ* hybridization.

A differential developmental regulation between males and females can also account for the differences found. The current model of adrenocortical homeostatic

maintenance claims that the cells with progenitor properties lie in the capsular and/or subcapsular region. These cells then differentiate during a centripetal migration into glomerulosa, fasciculata and reticularis, undergoing apoptosis in the boundary between the cortex and the medulla (140). We speculate that, in the more differentiated fasciculata cells, the transcription of the Task3 gene decreases. A testosterone dependent mechanism (a longer half-life of the Task3 protein, for example) could support the membrane expression of the protein in *zona fasciculata* cells.

5.2 Task3 channels contribute to the major K^+ current in adrenocortical cells and provide them with their unique K^+ sensibility

We and others (67; 75; 141) have observed that adrenocortical cells function like a potassium sensitive electrode in regard to their membrane voltage. Thus, they are hyperpolarized under control conditions and the membrane potential follows the changes in $[K^+]_o$. These cells behave similarly to the "ideal cell" predicted by the Nernst equation. Indeed, the V_m was linearly related to the log of the $[K^+]_o$ (slope of the regression = 43.5 mV per 10-fold change; R^2=0.988). On the other hand, Task3$^{-/-}$ adrenocortical cells are strongly depolarized under control conditions and the V_m do not depend on the $[K^+]_o$ (see Figure 4.5). Altogether these observations lead us to the conclusion that Task3$^{-/-}$ adrenocortical primary cells exhibit an impaired K^+ conductance and therefore K^+ sensitivity. These results were confirmed by measuring the cytoplasmic Ca^{2+} signal that results from $[K^+]_o$ increase (see Figure 4.6 and Figure 4.7).

Given the availability of similar studies on Task1$^{-/-}$ mice it is possible to further speculate on the particular contribution of each channel to the adrenocortical K^+ conductance. Here we report that Task3 deletion leads to a depolarization of approximately 27 mV at $[K^+]_o$ of 3.8 mM when compared to wild type animals. Conversely, Heitzmann and co-workers (66) reported a depolarization of approximately 7 mV inTask1$^{-/-}$ adrenocortical primary cells compared to wild type through a similar approach. It is noticeable that the contribution of Task3 to the resting potassium conductance of mouse adrenocortical primary cells is thus larger than that of Task1.

In this work we report a novel method to measure the intracellular Ca^{2+} signaling by loading freshly prepared adrenal slices with the Ca^{2+} sensitive dye Fluo-4 AM. Through this means, it was possible to confirm the impairment of the potassium sensitivity observed previously in Task3$^{-/-}$ adrenocortical primary cells (see Figure 4.6 and Figure 4.7). This is a highly valuable method which enables at the same time the unequivocal identification of *zona glomerulosa* cells, and the measurement of $[Ca^{2+}]_i$ changes in a more physiological scenario.

In the context of the accepted model of the regulation of aldosterone secretion, one would expect a severe disruption in the aldosterone secretion as a consequence of the deletion of Task3. Drastically depolarized glomerulosa cells would be expected to have an increased T and probably also L-type voltage gated Ca^{2+} channels activity. This would promote an increase of $[Ca^{2+}]_i$, even under control conditions, leading to a greater aldosterone secretion.

Surprisingly, the $[Ca^{2+}]_i$ baseline was similar in Task3$^{+/+}$ and Task3$^{-/-}$ adrenocortical primary cells, as measured by Fura-2 AM (see Figure 4.6). On the other hand, Task3$^{-/-}$ glomerulosa cells from freshly prepared adrenal slices exhibit a more frequent spontaneous oscillations of $[Ca^{2+}]_i$ than their Task3$^{+/+}$ counterparts (see Figure 4.7 and Figure 4.10). It is tempting to hypothesize that this bursting activity is an evidence of an increased activity of voltage gated Ca^{2+} channels, presumably of L-type. Evidences for this hypothesis are given by the fact that when Task3$^{+/+}$ cells are subjected to 7.6 mM of $[K^+]_o$, and thus depolarize to -65 mV, still they do not exhibit such bursts (see Figure 4.7). This V_m is still far from the -50 mV proposed by Cohen and co-workers (64) as a threshold to trigger important Ca^{2+} currents through L-type Ca^{2+} channels. On the other hand, Task3$^{-/-}$ cells exhibit a V_m of -47.82 ± 2.77 mV under resting conditions, allowing L-type channel activity.

However, it seems that these transient augmentations of $[Ca^{2+}]_i$ in Task3$^{-/-}$ glomerulosa cells are not enough to elicit supra-basal levels of aldosterone secretion; since the perifused adrenal glands from both genotypes secrete similar amounts of aldosterone under control conditions (see Figure 4.8). Furthermore, the impaired K^+ sensitivity observed in Task3$^{-/-}$ adrenocortical cells and slices is not reflected at the level of aldosterone secretion when looking at the whole organ. Task3$^{-/-}$ glands exhibit – if some - only minor differences comparatively to Task3$^{+/+}$ glands in terms of aldosterone secretion as a consequence of $[K^+]_o$ increase. As follows, the current model of the

regulation of aldosterone secretion fails to explain these results. It is still possible that different cells and not exclusively glomerulosa cells, are able to sense the $[K^+]_o$ and somehow transmit a secretory signal to aldosterone producing cells. A plethora of paracrine factors such as catecholamines (142-144), neuropeptides (145-147), intra-adrenal RAS (44; 148; 149) have been described to promote aldosterone secretion. Moreover, it has also been proposed that adrenal glomerulosa cells have only a minor impact on the *de novo* synthesis of aldosterone (150). According to this theory, their main function is to convert the corticosterone produced in *zona fasciculata* into aldosterone. We (data not show) and others (151) observed that upon *zona fasciculata* stimulation by typical aldosterone secretagogues such as K^+ and AngII, corticosterone secretion was increased too. All these hypotheses require an intact adrenal architecture. Therefore, the availability of zone-specific cell markers would allow the culture of pure cell populations and the study of possible interactions. For instance, the neural cell adhesion molecule CD56 has been recently used to isolate human *zona glomerulosa* cells (152). This and other zone-specific markers would be probably useful for further investigations.

5.3 The cellular response to AngII is altered in adrenocortical slices and primary cells

AngII promoted a strong depolarization and a decrease of outward currents in $Task3^{+/+}$ adrenocortical primary cells. On the other hand, $Task3^{-/-}$ cells exhibited a transient hyperpolarization followed by a slight depolarization as a consequence of AngII application (see Figure 4.9). These findings can be explained by the presence of large-conductance Ca^{2+} dependent MaxiK channels (107; 153). Indeed, we were able to measure putative MaxiK currents in cell attached and excised patches (inside-out) (preliminary data, not shown). The activation of MaxiK channels has been proposed to limit the depolarization triggered by AngII and hyperkalemia in glomerulosa cells and consequently the production of aldosterone (85). MaxiK channels have also been proposed to be involved in the inhibition of aldosterone secretion by ANP (84).

Our findings also provide indirect evidences of the contribution of Task1 homodimers to whole cell conductance. A late depolarization - compared to the resting V_m - was observed in $Task3^{-/-}$ cells as a result of AngII action. Furthermore, it was still possible to depolarize $Task3^{-/-}$ primary cells by some 20 mV upon extracellular acidification, very

similar to the depolarization obtained in Task3$^{+/+}$ cells. On the other hand, Heitzmann and co-workers (66) observed a depolarization of approximately 5 mV in Task1$^{-/-}$ adrenocortical cells upon extracellular acidification. These evidences are in agreement with the previous findings that Task3 channels (119) are less sensitive to pH than Task1 channels (118).

Not only the electrophysiological characteristics, but also the cytoplasmic Ca^{2+} response of Task3$^{-/-}$ glomerulosa cells upon the application of AngII was altered in comparison to Task3$^{+/+}$ cells (Figure 4.10). AngII caused an increase in $[Ca^{2+}]_i$ in Task3$^{+/+}$ glomerulosa cells from adrenal slices. Although the effect was heterogeneous, bursting $[Ca^{2+}]_i$ increases were a common feature. On the other hand, in Task3$^{-/-}$ cells the cytoplasmic Ca^{2+} bursting activity was also present, but as discussed previously, it also appeared in non-stimulated cells. It seems that the initial Ca^{2+} release from the ER is conserved in these cells, but the sustained phase - supported by the influx through voltage activated Ca^{2+} channels - is altered. Interestingly, the bursting cytoplasmic Ca^{2+} activity was transiently silenced in a group of Task3$^{-/-}$ glomerulosa cells after AngII addition. This phenomenon can be explained by the inactivation of the voltage gated Ca^{2+} channels due to the transient hyperpolarization observed in the primary cultured cells.

5.4 The physiological regulation of aldosterone secretion fails in Task3$^{-/-}$ mice

Although the impact of Task3 deletion is remarkable given the severe impairment of V_m, the reduced $[K^+]_o$ sensitivity and the reduced cytoplasmic Ca^{2+} signaling in adrenocortical cells, the overall phenotype of the Task3$^{-/-}$ mice is surprisingly mild. Heitzmann and co-workers (66) described a sex dependent dezonation of aldosterone synthase as a consequence of the deletion of Task1. This Task1 deletion depolarized the adrenocortical cells by approximately 7 mV. Here we described a far stronger depolarization with no consequences in aldosterone synthase localization (see Figure 4.4). It is tempting to hypothesize that the dezonation exhibited by Task1$^{-/-}$ females is related to a yet unknown developmental function of Task1, rather than to its channel properties.

Despite their depolarized adrenocortical cells, the plasma aldosterone concentrations of Task3$^{-/-}$ mice subjected to control diet are similar to those of Task3$^{+/+}$ animals. However, Task3$^{-/-}$ mice failed to increase their aldosterone secretion normally when subjected to K^+ rich diet (see Figure 4.11). This phenotype resembles the impaired K^+ sensitivity observed in adrenocortical primary cells and adrenal slices.

Numerous evidences support the conclusion that Task3$^{-/-}$ mice exhibit partial autonomy with regard to the adrenal secretion of aldosterone. At a cellular level the depolarized V_m and the altered cytoplasmic Ca^{2+} signaling under control conditions support this hypothesis. At the organism level, Task3$^{-/-}$ mice exhibit a depressed renin activity when subjected to control diet. This might counteract the relative autonomy of basal aldosterone secretion leading to a compensated state of autonomy. After Na^+ deprivation, the RAS is able to stimulate aldosterone secretion but this regulatory pathway fails when the mice are subjected to Na^+ rich diet. We speculate that this is related to the impossibility to further reduce aldosterone secretion below the autonomous basal level.

In any case, it seems clear that many compensatory mechanisms are involved in the regulation of aldosterone secretion in Task3$^{-/-}$ mice. Despite the described effects of Task3 deletion, these mice exhibit a normal mean arterial pressure (data not shown). However, preliminary results obtained by telemetric monitoring of the blood pressure point to a deregulation of circadian rhythms observed in Task3$^{+/+}$ mice.

5.5 Future directions

Our future research should be directed towards answering questions like:

- Why is the phenotype of Task3$^{-/-}$ mice only mild, despite the severe cellular impairment?
- Which mechanisms are supporting the adrenal *ex vivo* $[K^+]_o$ sensibility?
- Are Task3 defects involved in human pathologies?

We propose to address these and other questions by:

- Investigating the *ex vivo* response of the adrenal gland to AngII.

- Examining the role of ACTH in the control of aldosterone secretion and blood pressure in Task3$^{-/-}$ animals.
- Exploring in detail the blood electrolytes concentrations and arterial pressure of Task3$^{-/-}$ mice.
- Developing a setup that allows electrophysiological measurements in tissue slices.
- Studying in detail the role of K_2P channels for the dynamics of the adrenal gland development and zonation in mice.

6 References

1. Kearney PM, Whelton M, Reynolds K, Muntner P, Whelton PK, He J. Global burden of hypertension: analysis of worldwide data. Lancet. 2005; 365(9455):217-23.

2. Rossi GP, Bernini G, Caliumi C, Desideri G, Fabris B, Ferri C, et al. A prospective study of the prevalence of primary aldosteronism in 1,125 hypertensive patients. Journal of the American College of Cardiology. 2006 Dec; 48(11):2293-300.

3. Douma S, Petidis K, Doumas M, Papaefthimiou P, Triantafyllou A, Kartali N, et al. Prevalence of primary hyperaldosteronism in resistant hypertension: a retrospective observational study. Lancet. 2008 Jun; 371(9628):1921-6.

4. Westerdahl C, Bergenfelz A, Isaksson A, Nerbrand C, Valdemarsson S. Primary aldosteronism among newly diagnosed and untreated hypertensive patients in a Swedish primary care area. Scandinavian Journal of Primary Health Care. 2011 Mar; 29(1):57-62.

5. Funder JW, Carey RM, Fardella C, Gomez-Sanchez CE, Mantero F, Stowasser M, et al. Case detection, diagnosis, and treatment of patients with primary aldosteronism: an endocrine society clinical practice guideline. The Journal of Clinical Endocrinology and Metabolism. 2008 Sep; 93(9):3266-81.

6. Gomez-Sanchez CE. Aldosterone Biosynthesis in the Rat Brain. Endocrinology. 1997 Aug; 138(8):3369-3373.

7. Takeda Y, Yoneda T, Demura M, Miyamori I, Mabuchi H. Cardiac aldosterone production in genetically hypertensive rats. Hypertension. 2000 Oct; 36(4):495-500.

8. Keegan CE, Hammer GD. Recent insights into organogenesis of the adrenal cortex. Trends in Endocrinology and Metabolism. 2002 Jul; 13(5):200-8.

9. Hershkovitz L, Beuschlein F, Klammer S, Krup M, Weinstein Y. Adrenal 20alpha-hydroxysteroid dehydrogenase in the mouse catabolizes progesterone and 11-deoxycorticosterone and is restricted to the X-zone. Endocrinology. 2007 Mar; 148(3):976-88.

10. Vahouny G, Dennis P, Chanderbhan R, Fiskum G, Noland B, Scallen T. Sterol carrier protein2 (SCP2)-mediated transfer of cholesterol to mitochondrial inner membranes. Biochemical and Biophysical Research Communications. 1984 Jul; 122(2):509-515.

11. Simard J, Ricketts M-L, Gingras S, Soucy P, Feltus FA, Melner MH. Molecular biology of the 3beta-hydroxysteroid dehydrogenase/delta5-delta4 isomerase gene family. Endocrine Reviews. 2005 Jun; 26(4):525-82.

12. Doi M, Takahashi Y, Komatsu R, Yamazaki F, Yamada H, Haraguchi S, et al. Salt-sensitive hypertension in circadian clock-deficient Cry-null mice involves dysregulated adrenal Hsd3b6. Nature medicine. 2010 Jan; 16(1):67-74.

13. Spyroglou A, Manolopoulou J, Wagner S, Bidlingmaier M, Reincke M, Beuschlein F. Short term regulation of aldosterone secretion after stimulation and suppression experiments in mice. Journal of molecular endocrinology. 2009 May; 42(5):407-13.

14. Soundararajan R, Pearce D, Hughey RP, Kleyman TR. Role of epithelial sodium channels and their regulators in hypertension. The Journal of Biological Chemistry. 2010 Jul; 285(40):30363-30369.

15. Connell JMC, Davies E. The new biology of aldosterone. The Journal of Endocrinology. 2005 Jul; 186(1):1-20.

16. Thomas W, Harvey BJ. Mechanisms underlying rapid aldosterone effects in the kidney. Annual Review of Rhysiology. 2011 Mar 17; 73335-57.

17. Zecevic M, Heitzmann D, Camargo SMR, Verrey F. SGK1 increases Na,K-ATP cell-surface expression and function in Xenopus laevis oocytes. Pflügers Archiv : European Rournal of Physiology. 2004 Apr; 448(1):29-35.

18. Alvarez de la Rosa D, Gimenez I, Forbush B, Canessa CM. SGK1 activates Na^+-K^+-ATPase in amphibian renal epithelial cells. American Journal of Physiology. Cell Physiology. 2006 Feb; 290(2):C492-8.

19. Yoo D, Kim BY, Campo C, Nance L, King A, Maouyo D, et al. Cell surface expression of the ROMK (Kir 1.1) channel is regulated by the aldosterone-induced kinase, SGK-1, and protein kinase A. The Journal of Biological Chemistry. 2003 Jun 20; 278(25):23066-75.

20. Wang W-H, Yue P, Sun P, Lin D-H. Regulation and function of potassium channels in aldosterone-sensitive distal nephron. Current opinion in Nephrology and Hypertension. 2010 Sep; 19(5):463-70.

21. Gekle M, Golenhofen N, Oberleithner H, Silbernagl S. Rapid activation of Na^+/H^+ exchange by aldosterone in renal epithelial cells requires Ca^{2+} and stimulation of a plasma membrane proton conductance. Proceedings of the National Academy of Sciences of the United States of America. 1996 Sep 17; 93(19):10500-4.

22. Haseroth K, Gerdes D, Berger S, Feuring M, Günther a, Herbst C, et al. Rapid nongenomic effects of aldosterone in mineralocorticoid-receptor-knockout mice. Biochemical and Biophysical Research Communications. 1999 Dec 9; 266(1):257-61.

23. Pearce D. SGK1 regulation of epithelial sodium transport. Cellular Physiology and Biochemistry : International Journal of Experimental Cellular Physiology, Biochemistry, and Pharmacology. 2003 Jan; 13(1):13-20.

24. Fejes-Tóth G, Frindt G, Náray-Fejes-Tóth A, Palmer LG. Epithelial Na^+ channel activation and processing in mice lacking SGK1. American Journal of Physiology. Renal Physiology. 2008 Jun; 294(6):F1298-305.

25. Gekle M, Freudinger R, Mildenberger S, Silbernagl S. Rapid actions of aldosterone on cells from renal epithelium: the possible role of EGF-receptor signaling. Steroids. 2002 May; 67(6):499-504.

26. Koppel H. Nongenomic Effects of Aldosterone on Human Renal Cells. Journal of Clinical Endocrinology & Metabolism. 2003 Mar 1;88(3):1297-1302.

27. Christ M, Meyer C, Sippel K, Wehling M. Rapid aldosterone signaling in vascular smooth muscle cells: involvement of phospholipase C, diacylglycerol and protein kinase C alpha. Biochemical and Biophysical Research Communications. 1995 Aug 4;213(1):123-9.

28. McEneaney V, Harvey BJ, Thomas W. Aldosterone rapidly activates protein kinase D via a mineralocorticoid receptor/EGFR trans-activation pathway in the M1 kidney CCD cell line. The Journal of Steroid Biochemistry and Molecular Biology. 2007; 107(3-5):180-90.

29. Thomas W, McEneaney V, Harvey BJ. Aldosterone-stimulated PKC signaling cascades: from receptor to effector. Biochemical Society Transactions. 2007 Nov; 35(Pt 5):1049-51.

30. Li D, Wang Z, Sun P, Jin Y, Lin D-H, Hebert SC, et al. Inhibition of MAPK stimulates the Ca^{2+}-dependent big-conductance K channels in cortical collecting duct. Proceedings of the National Academy of Sciences of the United States of America. 2006 Dec 19;103(51):19569-74.

31. Doolan CM, Harvey BJ. Modulation of cytosolic protein kinase C and calcium ion activity by steroid hormones in rat distal colon. The Journal of Biological Chemistry. 1996 Apr 12;271(15):8763-7.

32. Gekle M, Silbernagl S, Oberleithner H. The mineralocorticoid aldosterone activates a proton conductance in cultured kidney cells. The American Journal of Physiology. 1997 Nov; 273(5 Pt 1):C1673-8.

33. Estilo G, Liu W, Pastor-Soler N, Mitchell P, Carattino MD, Kleyman TR, et al. Effect of aldosterone on BK channel expression in mammalian cortical collecting duct. American Journal of Physiology. Renal Physiology. 2008 Sep; 295(3):F780-8.

34. Hoorn EJ, Nelson JH, McCormick J a, Ellison DH. The WNK Kinase Network Regulating Sodium, Potassium, and Blood Pressure. Journal of the American Society of Nephrology : JASN. 2011 Apr; 22(4):605-14.

35. Rinehart J, Kahle KT, Los Heros P de, Vazquez N, Meade P, Wilson FH, et al. WNK3 kinase is a positive regulator of NKCC2 and NCC, renal cation-Cl^- cotransporters required for normal blood pressure homeostasis. Proceedings of

the National Academy of Sciences of the United States of America. 2005 Nov 15;102(46):16777-82.

36. Náray-Fejes-Tóth A, Snyder PM, Fejes-Tóth G. The kidney-specific WNK1 isoform is induced by aldosterone and stimulates epithelial sodium channel-mediated Na^+ transport. Proceedings of the National Academy of Sciences of the United States of America. 2004 Dec 14;101(50):17434-9.

37. Yang C-ling, Angell J, Mitchell R, Ellison DH. WNK kinases regulate thiazide-sensitive Na-Cl cotransport. The Journal of Clinical Investigation. 2003 Apr; 111(7):1039-45.

38. Fels J, Oberleithner H, Kusche-Vihrog K. Ménage à trois: Aldosterone, sodium and nitric oxide in vascular endothelium. Biochimica et Biophysica Acta. 2010 Mar 17;1802(12):1193-1202.

39. Funder JW. The nongenomic actions of aldosterone. Endocrine Reviews. 2005 May; 26(3):313-21.

40. Geerling JC, Loewy AD. Central regulation of sodium appetite. Experimental Physiology. 2008 Feb; 93(2):177-209.

41. Geerling JC, Engeland WC, Kawata M, Loewy AD. Aldosterone target neurons in the nucleus tractus solitarius drive sodium appetite. The Journal of Neuroscience : The Official Journal of the Society for Neuroscience. 2006 Jan 11;26(2):411-7.

42. Brilla CG, Pick R, Tan LB, Janicki JS, Weber KT. Remodeling of the rat right and left ventricles in experimental hypertension. Circulation Research. 1990 Dec; 67(6):1355-64.

43. Klug D, Robert V, Swynghedauw B. Role of mechanical and hormonal factors in cardiac remodeling and the biologic limits of myocardial adaptation. The American Journal of Cardiology. 1993 Jan 21;71(3):46A-54A.

44. Spät A, Hunyady L. Control of aldosterone secretion: a model for convergence in cellular signaling pathways. Physiological Reviews. 2004 Apr; 84(2):489-539.

45. Ito M, Oliverio MI, Mannon PJ, Best CF, Maeda N, Smithies O, et al. Regulation of blood pressure by the type 1A angiotensin II receptor gene. Proceedings of the National Academy of Sciences of the United States of America. 1995 Apr; 92(8):3521-5.

46. Oliverio MI, Best CF, Smithies O, Coffman TM. Regulation of sodium balance and blood pressure by the AT(1A) receptor for angiotensin II. Hypertension. 2000 Feb; 35(2):550-4.

47. Dinh DT, Frauman a G, Johnston CI, Fabiani ME. Angiotensin receptors: distribution, signaling and function. Clinical Science (London, England : 1979). 2001 May; 100(5):481-92.

48. Wynne BM, Chiao C-W, Webb RC. Vascular Smooth Muscle Cell Signaling Mechanisms for Contraction to Angiotensin II and Endothelin-1. Journal of the American Society of Hypertension : JASH. 2010; 3(2):84-95.

49. Giacché M, Vuagnat a, Hunt SC, Hopkins PN, Fisher ND, Azizi M, et al. Aldosterone stimulation by angiotensin II : influence of gender, plasma renin, and familial resemblance. Hypertension. 2000 Mar; 35(3):710-6.

50. Rincon Garriz JM, Suarez C, Capponi AM. c-Fos mediates angiotensin II-induced aldosterone production and protein synthesis in bovine adrenal glomerulosa cells. Endocrinology. 2009 Mar; 150(3):1294-302.

51. Capponi AM. The control by angiotensin II of cholesterol supply for aldosterone biosynthesis. Molecular and Cellular Endocrinology. 2004 Mar; 217(1-2):113-8.

52. Gambaryan S, Butt E, Tas P, Smolenski A, Allolio B, Walter U. Regulation of aldosterone production from zona glomerulosa cells by ANG II and cAMP: evidence for PKA-independent activation of CaMK by cAMP. American Journal of Physiology. Endocrinology and Metabolism. 2006 Mar; 290(3):E423-33.

53. Nogueira EF, Xing Y, Morris C a V, Rainey WE. Role of angiotensin II-induced rapid response genes in the regulation of enzymes needed for aldosterone synthesis. Journal of Molecular Endocrinology. 2009 Apr; 42(4):319-30.

54. Nogueira EF, Vargas C a, Otis M, Gallo-Payet N, Bollag WB, Rainey WE. Angiotensin-II acute regulation of rapid response genes in human, bovine, and rat adrenocortical cells. Journal of Molecular Endocrinology. 2007 Dec; 39(6):365-74.

55. Romero DG, Plonczynski MW, Welsh BL, Gomez-Sanchez CE, Zhou MY, Gomez-Sanchez EP. Gene expression profile in rat adrenal zona glomerulosa cells stimulated with aldosterone secretagogues. Physiological Genomics. 2007 Dec; 32(1):117-27.

56. Moravec CS, Schluchter MD, Paranandi L, Czerska B, Stewart RW, Rosenkranz E, et al. Inotropic effects of angiotensin II on human cardiac muscle in vitro. Circulation. 1990 Dec; 82(6):1973-84.

57. Livett BG, Marley PD. Noncholinergic control of adrenal catecholamine secretion. Journal of Anatomy. 1993 Oct; 183 (Pt 2277-89.

58. Phillips MI. Functions of angiotensin in the central nervous system. Annual Review of Physiology. 1987 Jan; 49413-35.

59. Wolf G, Wenzel UO. Angiotensin II and cell cycle regulation. Hypertension. 2004 Apr; 43(4):693-8.

60. Belloni AS, Andreis PG, Macchi V, Gottardo G, Malendowicz LK, Nussdorfer GG. Distribution and functional significance of angiotensin-II AT1- and AT2-

receptor subtypes in the rat adrenal gland. Endocrine Research. 1998 Feb; 24(1):1-15.

61. Gutowski S, Smrcka a, Nowak L, Wu DG, Simon M, Sternweis PC. Antibodies to the alpha q subfamily of guanine nucleotide-binding regulatory protein alpha subunits attenuate activation of phosphatidylinositol 4,5-bisphosphate hydrolysis by hormones. The Journal of Biological Chemistry. 1991 Oct; 266(30):20519-24.

62. Mogami H, Zhang H, Suzuki Y, Urano T, Saito N, Kojima I, et al. Decoding of short-lived Ca^{2+}influx signals into long term substrate phosphorylation through activation of two distinct classes of protein kinase C. The Journal of Biological Chemistry. 2003 Mar; 278(11):9896-904.

63. Rössig L, Zólyomi a, Catt KJ, Balla T. Regulation of angiotensin II-stimulated Ca^{2+}oscillations by Ca^{2+}influx mechanisms in adrenal glomerulosa cells. The Journal of Biological Chemistry. 1996 Sep; 271(36):22063-9.

64. Cohen CJ, McCarthy RT, Barrett PQ, Rasmussen H. Ca channels in adrenal glomerulosa cells: K^+ and angiotensin II increase T-type Ca channel current. Proceedings of the National Academy of Sciences of the United States of America. 1988 Apr; 85(7):2412-6.

65. Davies L a, Hu C, Guagliardo N a, Sen N, Chen X, Talley EM, et al. TASK channel deletion in mice causes primary hyperaldosteronism. Proceedings of the National Academy of Sciences of the United States of America. 2008 Feb; 105(6):2203-8.

66. Heitzmann D, Derand R, Jungbauer S, Bandulik S, Sterner C, Schweda F, et al. Invalidation of TASK1 potassium channels disrupts adrenal gland zonation and mineralocorticoid homeostasis. The EMBO Journal. 2008 Jan; 27(1):179-87.

67. Spät A. Glomerulosa cell--a unique sensor of extracellular K^+ concentration. Molecular and Cellular Endocrinology. 2004 Mar; 217(1-2):23-6.

68. Czirják G, Enyedi P. TASK-3 dominates the background potassium conductance in rat adrenal glomerulosa cells. Molecular Endocrinology. 2002 Mar; 16(3):621-9.

69. Brenner T, O□Shaughnessy KM. Both TASK-3 and TREK-1 two-pore loop K channels are expressed in H295R cells and modulate their membrane potential and aldosterone secretion. American Journal of Physiology. Endocrinology and Metabolism. 2008 Dec; 295(6):E1480-6.

70. Czirják G, Fischer T, Spät A, Lesage F, Enyedi P. TASK (TWIK-related acid-sensitive K^+ channel) is expressed in glomerulosa cells of rat adrenal cortex and inhibited by angiotensin II. Molecular Endocrinology. 2000 Jun; 14(6):863-74.

71. Lotshaw DP. Biophysical, pharmacological, and functional characteristics of cloned and native mammalian two-pore domain K^+ channels. Cell Biochemistry and Biophysics. 2007 May; 47(2):209-256.

72. Chen X, Talley EM, Patel N, Gomis A, McIntire WE, Dong B, et al. Inhibition of a background potassium channel by Gq protein alpha-subunits. Proceedings of the National Academy of Sciences of the United States of America. 2006 Feb; 103(9):3422-7.

73. McCarthy RT, Isales C, Rasmussen H. T-type calcium channels in adrenal glomerulosa cells: GTP-dependent modulation by angiotensin II. Proceedings of the National Academy of Sciences of the United States of America. 1993 Apr; 90(8):3260-4.

74. Maturana a D, Casal a J, Demaurex N, Vallotton MB, Capponi a M, Rossier MF. Angiotensin II negatively modulates L-type calcium channels through a pertussis toxin-sensitive G protein in adrenal glomerulosa cells. The Journal of Biological Chemistry. 1999 Jul; 274(28):19943-8.

75. Lotshaw DP. Role of membrane depolarization and T-type Ca^{2+}channels in angiotensin II and K^{+} stimulated aldosterone secretion. Molecular and Cellular Endocrinology. 2001 Apr; 175(1-2):157-71.

76. Balla T, Holló Z, Várnai P, Spät A. Angiotensin II inhibits K(+)-induced Ca^{2+}signal generation in rat adrenal glomerulosa cells. The Biochemical Journal. 1991 Jan 15; 273(Pt 2)399-404.

77. Rohács T, Bagó a, Deák F, Hunyady L, Spät a. Capacitative Ca^{2+}influx in adrenal glomerulosa cells: possible role in angiotensin II response. The American Journal of Physiology. 1994 Nov; 267(5 Pt 1):C1246-52.

78. Ely J a, Ambroz C, Baukal a J, Christensen SB, Balla T, Catt KJ. Relationship between agonist- and thapsigargin-sensitive calcium pools in adrenal glomerulosa cells. Thapsigargin-induced Ca^{2+}mobilization and entry. The Journal of Biological Chemistry. 1991 Oct; 266(28):18635-41.

79. Cahalan MD. STIMulating store-operated Ca^{2+} entry. Nature Cell Biology. 2009 Jun; 11(6):669-77.

80. Huber a, Sander P, Gobert a, Bähner M, Hermann R, Paulsen R. The transient receptor potential protein (Trp), a putative store-operated Ca^{2+}channel essential for phosphoinositide-mediated photoreception, forms a signaling complex with NorpA, InaC and InaD. The EMBO Journal. 1996 Dec 16;15(24):7036-45.

81. Parekh AB, Putney JW. Store-operated calcium channels. Physiological Reviews. 2005 Apr; 85(2):757-810.

82. Philipp S, Trost C, Warnat J, Rautmann J, Himmerkus N, Schroth G, et al. TRP4 (CCE1) protein is part of native calcium release-activated Ca^{2+}-like channels in adrenal cells. The Journal of Biological Chemistry. 2000 Aug 4;275(31):23965-72.

83. Várnai P, Hunyady L, Balla T. STIM and Orai: the long-awaited constituents of store-operated calcium entry. Trends in Pharmacological Sciences. 2009 Mar; 30(3):118-28.

84. Ganz MB, Nee JJ, Isales CM, Barrett PQ. Atrial natriuretic peptide enhances activity of potassium conductance in adrenal glomerulosa cells. The American Journal of Physiology. 1994 May; 266(5 Pt 1):C1357-65.

85. Bandulik S, Penton D, Barhanin J, Warth R. TASK1 and TASK3 potassium channels: determinants of aldosterone secretion and adrenocortical zonation. Hormone and Metabolic Research. 2010 Jun; 42(6):450-7.

86. Chiu T, Santiskulvong C, Rozengurt E. ANG II stimulates PKC-dependent ERK activation, DNA synthesis, and cell division in intestinal epithelial cells. American journal of physiology. Gastrointestinal and Liver Physiology. 2003 Jul; 285(1):G1-11.

87. Christenson LK, Strauss JF. Steroidogenic acute regulatory protein: an update on its regulation and mechanism of action. Archives of Medical Research. 2001; 32(6):576-86.

88. Condon JC. Calmodulin-Dependent Kinase I Regulates Adrenal Cell Expression of Aldosterone Synthase. Endocrinology. 2002 Sep; 143(9):3651-3657.

89. Barrett PQ, Lu HK, Colbran R, Czernik A, Pancrazio JJ. Stimulation of unitary T-type Ca^{2+} channel currents by calmodulin-dependent protein kinase II. American journal of physiology. Cell Physiology. 2000 Dec; 279(6):C1694-703.

90. Shieh CC, Coghlan M, Sullivan JP, Gopalakrishnan M. Potassium channels: molecular defects, diseases, and therapeutic opportunities. Pharmacological Reviews. 2000 Dec; 52(4):557-94.

91. Choi M, Scholl UI, Yue P, Björklund P, Zhao B, Nelson-Williams C, et al. K^+ channel mutations in adrenal aldosterone-producing adenomas and hereditary hypertension. Science. 2011 Feb; 331(6018):768-72.

92. Been LF, Ralhan S, Wander GS, Mehra NK, Singh J, Mulvihill JJ, et al. Variants in KCNQ1 increase type II diabetes susceptibility in South Asians: a study of 3,310 subjects from India and the US. BMC Medical Genetics. 2011 Jan; 12(1):18.

93. Bockenhauer D, Feather S, Stanescu HC, Bandulik S, Zdebik A a, Reichold M, et al. Epilepsy, ataxia, sensorineural deafness, tubulopathy, and KCNJ10 mutations. The New England Journal of Medicine. 2009 May; 360(19):1960-70.

94. Bellocq C, Ginneken ACG van, Bezzina CR, Alders M, Escande D, Mannens MM a M, et al. Mutation in the KCNQ1 gene leading to the short QT-interval syndrome. Circulation. 2004 May; 109(20):2394-7.

95. Enyedi P, Czirják G. Molecular background of leak K^+ currents: two-pore domain potassium channels. Physiological Reviews. 2010 Apr; 90(2):559-605.

96. Bayliss D a, Sirois JE, Talley EM. The TASK family: two-pore domain background K^+ channels. Molecular Interventions. 2003 Jun; 3(4):205-19.

97. Czirják G, Enyedi P. Formation of functional heterodimers between the TASK-1 and TASK-3 two-pore domain potassium channel subunits. The Journal of Biological Chemistry. 2002 Feb; 277(7):5426-32.

98. Decher N, Maier M, Dittrich W, Gassenhuber J, Brüggemann a, Busch a E, et al. Characterization of TASK-4, a novel member of the pH-sensitive, two-pore domain potassium channel family. FEBS Letters. 2001 Mar; 492(1-2):84-9.

99. Kim D, Gnatenco C. TASK-5, a new member of the tandem-pore K(+) channel family. Biochemical and Biophysical Research Communications. 2001 Jun; 284(4):923-30.

100. Liu H, Enyeart J a, Enyeart JJ. Angiotensin II inhibits native bTREK-1 K^+ channels through a PLC-, kinase C-, and PIP2-independent pathway requiring ATP hydrolysis. American Journal of Physiology. Cell Physiology. 2007 Aug; 293(2):C682-95.

101. Enyeart J a, Danthi SJ, Enyeart JJ. TREK-1 K^+ channels couple angiotensin II receptors to membrane depolarization and aldosterone secretion in bovine adrenal glomerulosa cells. American Journal of Physiology. Endocrinology and Metabolism. 2004 Dec; 287(6):E1154-65.

102. Enyeart JJ, Xu L, Danthi S, Enyeart J a. An ACTH- and ATP-regulated background K^+ channel in adrenocortical cells is TREK-1. The Journal of Biological Chemistry. 2002 Dec; 277(51):49186-99.

103. Liu H, Enyeart J a, Enyeart JJ. ACTH inhibits bTREK-1 K^+ channels through multiple cAMP-dependent signaling pathways. The Journal of General Physiology. 2008 Aug; 132(2):279-94.

104. Enyeart J a, Danthi S, Enyeart JJ. Corticotropin induces the expression of TREK-1 mRNA and K^+ current in adrenocortical cells. Molecular pharmacology. 2003 Jul; 64(1):132-42.

105. Arrighi I, Bloch-Faure M, Grahammer F, Bleich M, Warth R, Mengual R, et al. Altered potassium balance and aldosterone secretion in a mouse model of human congenital long QT syndrome. Proceedings of the National Academy of Sciences of the United States of America. 2001 Jul; 98(15):8792-7.

106. Sarzani R, Pietrucci F, Francioni M, Salvi F, Letizia C, D□Erasmo E, et al. Expression of potassium channel isoforms mRNA in normal human adrenals and aldosterone-secreting adenomas. Journal of Endocrinological Investigation. 2006 Feb; 29(2):147-53.

107. Sausbier M, Arntz C, Bucurenciu I, Zhao H, Zhou X-B, Sausbier U, et al. Elevated blood pressure linked to primary hyperaldosteronism and impaired vasodilation in BK channel-deficient mice. Circulation. 2005 Jul; 112(1):60-8.

108. Xu H, Garver H, Galligan JJ, Fink GD. Large-conductance Ca^{2+}-activated K^+ channel β1-subunit knockout mice are not hypertensive. American journal of physiology. Heart and Circulatory Physiology. 2011 Feb; 300(2):H476-85.

109. Kanazirska MV, Vassilev PM, Quinn SJ, Tillotson DL, Williams GH. Single K^+ channels in adrenal zona glomerulosa cells. II. Inhibition by angiotensin II. The American Journal of Physiology. 1992 Oct; 263(4 Pt 1):E760-5.

110. Vassilev PM, Kanazirska MV, Quinn SJ, Tillotson DL, Williams GH. K^+ channels in adrenal zona glomerulosa cells. I. Characterization of distinct channel types. The American Journal of Physiology. 1992 Oct; 263(4 Pt 1):E752-9.

111. Lotshaw DP. Characterization of angiotensin II-regulated K^+ conductance in rat adrenal glomerulosa cells. The Journal of Membrane Biology. 1997 Apr; 156(3):261-77.

112. Lesage F, Guillemare E, Fink M, Duprat F, Lazdunski M, Romey G, et al. TWIK-1, a ubiquitous human weakly inward rectifying K^+ channel with a novel structure. The EMBO Journal. 1996 Mar; 15(5):1004-11.

113. Bayliss D a, Barrett PQ. Emerging roles for two-pore-domain potassium channels and their potential therapeutic impact. Trends in Pharmacological Sciences. 2008 Nov; 29(11):566-75.

114. Medhurst a D, Rennie G, Chapman CG, Meadows H, Duckworth MD, Kelsell RE, et al. Distribution analysis of human two pore domain potassium channels in tissues of the central nervous system and periphery. Brain research. Molecular Brain Research. 2001 Jan; 86(1-2):101-14.

115. Enyeart JJ, Danthi SJ, Liu H, Enyeart J a. Angiotensin II inhibits bTREK-1 K^+ channels in adrenocortical cells by separate Ca^{2+}- and ATP hydrolysis-dependent mechanisms. The Journal of Biological Chemistry. 2005 Sep; 280(35):30814-28.

116. Takemori S, Kominami S, Yamazaki T, Ikushiro S. Molecular mechanism of cytochrome P-450-dependent aldosterone biosynthesis in the adrenal cortex. Trends in Endocrinology and Metabolism. 1995 Oct; 6(8):267-73.

117. Rajan S, Wischmeyer E, Xin Liu G, Preisig-Müller R, Daut J, Karschin a, et al. TASK-3, a novel tandem pore domain acid-sensitive K^+ channel. An extracellular histiding as pH sensor. The Journal of Biological Chemistry. 2000 Jun; 275(22):16650-7.

118. Duprat F, Lesage F, Fink M, Reyes R, Heurteaux C, Lazdunski M. TASK, a human background K^+ channel to sense external pH variations near physiological pH. The EMBO Journal. 1997 Sep; 16(17):5464-71.

119. Kim Y, Bang H, Kim D. TASK-3, a new member of the tandem pore K(+) channel family. The Journal of Biological Chemistry. 2000 Mar 31;275(13):9340-7.

120. Patel a J, Honoré E, Lesage F, Fink M, Romey G, Lazdunski M. Inhalational anesthetics activate two-pore-domain background K^+ channels. Nature Neuroscience. 1999 May; 2(5):422-6.

121. Lazarenko RM, Willcox SC, Shu S, Berg AP, Jevtovic-Todorovic V, Talley EM, et al. Motoneuronal TASK channels contribute to immobilizing effects of inhalational general anesthetics. The Journal of Neuroscience : The Official Journal of the Society for Neuroscience. 2010 Jun; 30(22):7691-704.

122. Kang D, Han J, Talley EM, Bayliss D a, Kim D. Functional expression of TASK-1/TASK-3 heteromers in cerebellar granule cells. The Journal of Physiology. 2004 Jan; 554(Pt 1):64-77.

123. Clarke CE, Veale EL, Green PJ, Meadows HJ, Mathie A. Selective block of the human 2-P domain potassium channel, TASK-3, and the native leak potassium current, IKSO, by zinc. The Journal of Physiology. 2004 Oct; 560(Pt 1):51-62.

124. Luedi PP, Dietrich FS, Weidman JR, Bosko JM, Jirtle RL, Hartemink AJ. Computational and experimental identification of novel human imprinted genes. Genome Research. 2007 Dec; 17(12):1723-30.

125. Barel O, Shalev SA, Ofir R, Cohen A, Zlotogora J, Shorer Z, et al. Maternally inherited Birk Barel mental retardation dysmorphism syndrome caused by a mutation in the genomically imprinted potassium channel KCNK9. American Journal of Human Genetics. 2008 Aug; 83(2):193-9.

126. Ruf N, Bähring S, Galetzka D, Pliushch G, Luft FC, Nürnberg P, et al. Sequence-based bioinformatic prediction and QUASEP identify genomic imprinting of the KCNK9 potassium channel gene in mouse and human. Human Molecular Genetics. 2007 Nov 1;16(21):2591-9.

127. Guagliardo N a, Yao J, Bayliss D a, Barrett PQ. TASK channels are not required to mount an aldosterone secretory response to metabolic acidosis in mice. Molecular and Cellular Endocrinology. 2010 Nov;

128. Lifton RP, Dluhy RG, Powers M, Rich GM, Cook S, Ulick S, et al. A chimaeric 11 beta-hydroxylase/aldosterone synthase gene causes glucocorticoid-remediable aldosteronism and human hypertension. Nature. 1992 Jan; 355(6357):262-5.

129. Romero DG, Yanes LL, Rodriguez AF de, Plonczynski MW, Welsh BL, Reckelhoff JF, et al. Disabled-2 is expressed in adrenal zona glomerulosa and is involved in aldosterone secretion. Endocrinology. 2007 Jun; 148(6):2644-52.

130. Guyon A, Tardy MP, Rovère C, Nahon J-L, Barhanin J, Lesage F. Glucose inhibition persists in hypothalamic neurons lacking tandem-pore K^+ channels. The Journal of Neuroscience: The Official Journal of the Society for Neuroscience. 2009 Feb 25; 29(8):2528-33.

131. Sauer B, Henderson N. Site-specific DNA recombination in mammalian cells by the Cre recombinase of bacteriophage P1. Proceedings of the National Academy of Sciences of the United States of America. 1988 Jul; 85(14):5166-70.

132. Wotus C. Development of Adrenal Zonation in Fetal Rats Defined by Expression of Aldosterone Synthase and 11 -Hydroxylase. Endocrinology. 1998 Oct; 139(10):4397-4403.

133. Bielohuby M, Herbach N, Wanke R, Maser-Gluth C, Beuschlein F, Wolf E, et al. Growth analysis of the mouse adrenal gland from weaning to adulthood: time- and gender-dependent alterations of cell size and number in the cortical compartment. American Journal of Physiology. Endocrinology and Metabolism. 2007 Jul; 293(1):E139-46.

134. Tait SA, Tait JF. Personal History during their collaborative work on the isolation and elucidation of the structure of electrocortin (later aldosterone). Steroids. 1998 Sep; 63(9):440-53.

135. Tait SAS, Tait JF, Coghlan JP. The discovery, isolation and identification of aldosterone: reflections on emerging regulation and function. Molecular and Cellular Endocrinology. 2004 Mar 31;217(1-2):1-21.

136. Schteingart DE. The 50th anniversary of the identification of primary aldosteronism: a retrospective of the work of Jerome W. Conn. The Journal of Laboratory and Clinical Medicine. 2005 Jan; 145(1):12-6.

137. Perry JE, Stalvey JR. Gonadal steroids modulate adrenal fasciculata 3 beta-hydroxysteroid dehydrogenase-isomerase activity in mice. Biology of Reproduction. 1992 Jan; 46(1):73-82.

138. Stalvey JRD. Inhibition of 3beta-hydroxysteroid dehydrogenase-isomerase in mouse adrenal cells: a direct effect of testosterone. Steroids. 2002 Jul; 67(8):721-31.

139. Zubair M, Parker KL, Morohashi K-ichirou. Developmental links between the fetal and adult zones of the adrenal cortex revealed by lineage tracing. Molecular and Cellular Biology. 2008 Dec; 28(23):7030-40.

140. Kim AC, Barlaskar FM, Heaton JH, Else T, Kelly VR, Krill KT, et al. In search of adrenocortical stem and progenitor cells. Endocrine Reviews. 2009 May; 30(3):241-63.

141. Natke E, Kabela E. Electrical responses in cat adrenal cortex: possible relation to aldosterone secretion. The American Journal of Physiology. 1979 Aug; 237(2):E158-62.

142. Tóth IE, Vizi ES, Hinson JP, Vinson GP. Innervation of the adrenal cortex, its physiological relevance, with primary focus on the noradrenergic transmission. Microscopy Research and Technique. 1997 Mar; 36(6):534-45.

143. Capaldo a, Gay F, Valiante S, Laforgia V, Varano L. Effects of noradrenaline administration on the interrenal gland of the newt, Triturus carnifex: evidence of intra-adrenal paracrine interactions. Journal of Morphology. 2004 Jan; 259(1):33-40.

144. Szalay KS, Orsó E, Jurányi Z, Vinson GP, Vizi ES. Local non-synaptic modulation of aldosterone production by catecholamines and ATP in rat: implications for a direct neuronal fine tuning. Hormone and Metabolic Research. 1998; 30(6-7):323-8.

145. Whitworth EJ, Kosti O, Renshaw D, Hinson JP. Adrenal neuropeptides: regulation and interaction with ACTH and other adrenal regulators. Microscopy Research and Technique. 2003 Jun; 61(3):259-67.

146. Ehrhart-Bornstein M, Haidan a, Alesci S, Bornstein SR. Neurotransmitters and neuropeptides in the differential regulation of steroidogenesis in adrenocortical-chromaffin co-cultures. Endocrine Research. 2000 Nov; 26(4):833-42.

147. Bornstein SR, Ehrhart-Bornstein M, Scherbaum W a. Morphological and functional studies of the paracrine interaction between cortex and medulla in the adrenal gland. Microscopy Research and Technique. 1997 Mar 15;36(6):520-33.

148. Lavoie JL. Minireview: Overview of the Renin-Angiotensin System--An Endocrine and Paracrine System. Endocrinology. 2003 Jun; 144(6):2179-2183.

149. Vinson GP, Teja R, Ho MM, Hinson JP, Puddefoot JR. The role of the tissue renin-angiotensin system in the response of the rat adrenal to exogenous angiotensin II. The Journal of Endocrinology. 1998 Aug; 158(2):153-9.

150. Vinson GP. Glomerulosa function and aldosterone synthesis in the rat. Molecular and Cellular Endocrinology. 2004 Mar 31;217(1-2):59-65.

151. Robertson LM, Keith LD, Kendall JW. Potassium modulation of corticosterone secretion from perifused mouse adrenal cells. Metabolism: Clinical and Experimental. 1984 Aug; 33(8):703-9.

152. Caroccia B, Fassina A, Seccia TM, Recarti C, Petrelli L, Belloni AS, et al. Isolation of human adrenocortical aldosterone-producing cells by a novel immunomagnetic beads method. Endocrinology. 2010 Mar; 151(3):1375-80.

153. Grimm PR, Irsik DL, Settles DC, Holtzclaw JD, Sansom SC. Hypertension of Kcnmb1-/- is linked to deficient K secretion and aldosteronism. Proceedings of the National Academy of Sciences of the United States of America. 2009 Jul; 106(28):11800-5.

7 Supplements

Publications during PhD period

Reichold M, Zdebik AA, Lieberer E, Rapedius M, Schmidt K, Bandulik S, Sterner C, Tegtmeier I, **Penton D**, Baukrowitz T, Hulton SA, Witzgall R, Ben-Zeev B, Howie AJ, Kleta R, Bockenhauer D, Warth R. KCNJ10 gene mutations causing EAST syndrome (epilepsy, ataxia, sensorineural deafness, and tubulopathy) disrupt channel function. Proceedings of the National Academy of Sciences of the United States of America. 2010 Aug 10;107(32):14490-5

Bandulik S, **Penton D**, Barhanin J, Warth R. TASK1 and TASK3 potassium channels: determinants of aldosterone secretion and adrenocortical zonation. Hormone and Metabolic Research. 2010 Jun; 42(6):450-7

Penton D, Dandulik S, Schweda F, Haubs S, Tauber P, Reichold M, Cong LD, Vernerey D, Jeunemaitre X, Budde T, Lesage F, Zennaro MC, Barhanin J, Warth R. Task3 potassium channels: A determinant of aldosterone/renin ratio in mice and humans. Manuscript in preparation.

Presentations at Scientific conferences

“The role of Task3 potassium channels in the regulation of aldosterone secretion”, Oral presentation at the 37th Meeting of the International Aldosterone Conference. Boston (USA), 2-3 June. 2011.

“TASK3 potassium channels are involved in the regulation of aldosterone secretion in mice”, Oral presentation at the 90th Annual Meeting of the DPG. Regensburg (Germany), 26-29 March. 2011.

"TASK3 potassium channels are involved in the regulation of aldosterone secretion in mice", Poster presentation at the Joint Meeting of the Scandinavian and German Physiological Societies. Copenhagen (Denmark), 8-10 July. 2010.

"The role of Task3 potassium channels in the regulation of aldosterone secretion", Poster presentation at the 88th Annual Meeting of the DPG. Giessen (Germany), 22-25 March. 2009.

8 Acknowledgments

I want to express my gratitude to those people who helped me during this period of my education and life.

First I would like to thank my supervisor Prof. Dr. Richard Warth for the great experience that this PhD was for me. Through his guidance I discovered the fascinating world of physiology, which still keeps me trapped. He showed me that science can be at the same time sacrifice and fun; self improvement and friendship, and always challenging. Thank you very much!

I also want to thank Dr. Sascha Bandulik for his help, scientific guidance and fruitful discussions. To Dr. Markus Reichold, a special thanks for introducing me into electrophysiology (and for being so funny and comprehensive). Special thanks also to Evi, “Felipe”, Carste(te)n, Sophia, Maria, Ines, Karolin and Christina for all the help and for making the lab a unique place of joy.

I want to thank Prof. Dr. Jacques Barhanin for the scientific and personal advices as well as for his contribution to this work.

I would like to thank the staff from the “Mechanische Werkstatt Biologie” for making my craziest ideas technically possible.

Muchas gracias a René, sin su ayuda este trabajo hubiera quedado sólo en un sueño.

Un millón de gracias a Janet y a Abel, por su amistad y por la paciencia para leer y corregir este manuscrito.

Thank you Lesly, Sylvia (Kika), Diana, Nestor, Aim, Nadine, Arthur, Inna and Joana Almaça, for making my life easier in Germany.

Muchas gracias a Raquel por todo y por hacerme soñar. Obrigado à sua família por ser também a minha.

Esta tesis es mi pequeño regalo para mis padres, por todo su amor.

Para Diego es todo el universo.